MECHANICAL DESIGN OF SPICULE-REINFORCED CONNECTIVE TISSUE: STIFFNESS

By M. A. R. KOEHL

Department of Zoology, University of California, Berkeley, California 94720

SUMMARY

Many animals from different phyla have, embedded in their pliable connective tissues, small bits of stiff material known as spicules. The tensile behaviour of spicule-reinforced connective tissues from various cnidarians and sponges, as well as of model spiculated 'tissues', is here investigated in order to elucidate the effects on mechanical properties of spicule size and shape, and of their packing density and orientation within a tissue. The main conclusions are:

1. Spicules increase the stiffness of pliable connective tissues probably by mechanisms analogous to those by which filler particles stiffen deformable polymers – local strain amplification, and interference with molecular rearrangement in response to a load.

2. The greater the volume fraction of spicules, the stiffer the tissue.

3. The greater the surface area of spicules per volume of tissue, the stiffer the tissue. Thus, a given volume of spicules of high surface-area-to-volume-ratio (S/V) have a greater stiffening effect than does an equal volume of spicules of low S/V. Furthermore, a high volume fraction of large spicules in a tissue can have the same stiffening effect as a lower volume fraction of smaller spicules.

4. Spicules that are anisometric in shape have a greater stiffening effect parallel to their long axes.

5. Spicules with very high aspect ratios appear to act like reinforcing fibres – stress is transferred by shearing from the pliable matrix to the stiff fibres, which thus bear in tension part of the load on the composite.

6. Spicule-reinforced tissues exhibit stress-softening behaviour, which is more pronounced in heavily spiculated tissues.

INTRODUCTION

Small pieces of calcareous or siliceous material are embedded in the connective tissues of numerous animals from different phyla. Examples of such rigid particles in soft biological materials include the spicules of sponges, the sclerites of cnidarians, the ossicles of echinoderms, the spicules in some chitons (molluscs), stalked barnacles (arthropods), and ascidians (urochordates), and even the mineral deposits in the connective tissues of humans suffering from ailments such as osteoarthritis, calciferous tendonitis and bursitis, and gout. For ease of discussion, I shall refer to all small, stiff inclusions in soft biological materials as 'spicules'.

Spicules have been described as playing some role in mechanical support and/or as serving as predator-deterrents (e.g. Currey, 1970; Wainwright *et al.* 1976; Jackson, 1977; Berquist, 1978). In spite of their broad occurrence in the animal kingdom, however, the mechanical functions of spicules are poorly understood. In animals where spicules abut on each other, they are no doubt basically compressive skeletal elements. In some systems, such as starfish (Eylers, 1976), the small rigid elements are associated with muscles as well as connective tissue and essentially function as small bones. In other systems, such as lychnisc sponges (Reif & Robinson, 1976) and *Melithaea* (octocoral) stalks (Muzik & Wainwright, 1977), spicules appear to act like the struts of braced frameworks; the rigidity or flexibility of such braced frameworks depends on the arrangement of struts and on the deformability of the material joining them together (Wainwright *et al.* 1976).

What, if any, mechanical roles do spicules play in tissues in which they do not abut on each other? The structure of such spiculated tissues suggests that their mechanical behaviour may be analogous to that of man-made 'filled polymers', pliable materials reinforced with small, rigid inclusions.

The purpose of this study was to describe the tensile mechanical behaviour of spiculated tissues and to determine whether such tissues display the mechanical properties characteristic of filled polymers. A further purpose of this study was to explore the mechanical effects of spicule size, shape, and packing within connective tissues.

MATERIALS AND METHODS

Mechanical testing of spiculated tissues

Mechanical tests were conducted on fresh spiculated tissue from the sponges and cnidarians listed in Table 1. The animals were kept in aerated sea water aquaria at 10 °C (animals from Scotland) or at 20 °C (animals from the Red Sea). The *Alcyonium digitatum* were fed brine shrimp nauplii twice weekly; all other animals were not fed, but were used within a week of being collected. Alcyonacean colonies were anaesthetized overnight at 10 °C (or 20 °C) in solutions of 20% $MgSO_4.7H_2O$ one to one with sea water (Pantin, 1964) until polyps pinched with forceps did not contract. Strips of spicule-containing connective tissue ('coenenchyme') were cut from colonies with a scalpel and kept in anaesthetic at 10 °C (or 20 °C) for several hours until subjected to mechanical testing. Strips cut with a scalpel from sponges were kept in sea water at 10 °C until tested.

The cross-sectional area of each strip was determined by cutting a section off each end of the strip, mounting the sections in anaesthetic on microscope slides, tracing their perimeters and holes onto paper using a camera lucida on a compound microscope, cutting out and weighing the paper 'cross-sections', converting the weights to areas (to the nearest 0·01 mm^2) and taking the mean of the two areas (the standard error, S.E., for such pairs of cross sections was $\leq \pm 5$%). When such area determinations were repeated for sections at three successive 3 h intervals, no significant change in area with time was observed.

Tissue strips were gripped in spring-loaded clamps for mechanical testing and the length of each specimen between the grips was measured to the nearest 0·1 mm using

Table 1. *Spiculated tissues*

Source of tissue	Spicule composition*	Volume fraction of spicules $\pm$ S.D., n
Phylum Cnidaria		
Class Athozoa, Order Alcyonacea		
Alcyonium digitatum (L.)		
Outer coenenchyme	C	$0\cdot12\pm0\cdot04$, 6
Inner coenenchyme	C	$0\cdot12\pm0\cdot02$, 6
Dendronephtya (Dendronephyta) *hemprichi* (Klunzinger)†		
Sterile stalk	C	$0\cdot18\pm0\cdot02$, 3
Sarcophyton glaucum (Quoy and Gaimard)†		
Sterile stalk	C	$0\cdot36\pm0\cdot16$, 6
Phylum Porifera		
Class Demospongiae, Subclass Monoaxnida		
Suberites domuncula (Olivi)	S	$0\cdot14\pm0\cdot03$, 3
Hymeniacidon sanguinea (Grant)	S	$0\cdot05\pm0\cdot01$, 3
Class Calcarea		
Sycon ciliatum (Fabricius)	C	$0\cdot02\pm0\cdot002$, 3
Grantia compressa (Fabricius)	C	$0\cdot06\pm0\cdot01$, 3

* C = calcium carbonate, S = silicon dioxide; (Brown, 1975).
† Collected from the Red Sea. (All other animals were collected from the Firth of Clyde, Scotland.)

callipers. The surfaces of each specimen that would have come in contact with the grips were protected by squares of paper towel glued to the specimen with cyano-acrylate contact cement (Loctite Superbinder 496).

Strips of tissue were pulled at various rates in an Instron Universal Testing Instrument (Model TM-M) that simultaneously measured force (s.e. $= \pm 0\cdot5$ %) and extension (s.e. $= \pm 0\cdot25$ %). Data from specimens extended at a rate of 50 cm.min^{-1} was recorded by photographing the tracing on an oscilloscope (Tetronix 5103N oscilloscope system with a 5A22N differential amplifier for the force signal and a 5B10N time base amplifier for extension). Data from specimens pulled more slowly was recorded using the Instron's pen recorder. Plots of stress (σ, force per cross-sectional area) versus extension ratio (λ, ratio of extended length of the specimen to its original length) were made. The slope of the straight portion of each such stress-extension curve was taken to be the modulus of elasticity (E, a measure of stiffness) for that specimen.

Cyclic stress-extension tests were also performed using the Instron. Specimens were pulled at a given rate to a given load, immediately returned at the same rate to their original length, immediately pulled again to a greater load and returned, and so on.

Stress-relaxation tests were performed using the Instron. Specimens were rapidly stretched (strain rate, $\dot{\varepsilon} = 0\cdot3$ s^{-1}, where $\dot{\varepsilon} = \Delta L/tL_0$, where ΔL is the change in length of the specimen at time t, and L_0 is the original length of the specimen) to known lengths and then held; the force required to hold the specimen at that length was measured through time. Time-dependent elastic moduli ($E(t)$) were calculated,

$$E(t) = \frac{\sigma(t)}{\Delta L/L_0},$$

where $\sigma(t)$ is the stress in the tissue at time t. During stress-relaxation tests, specimens were submerged in a bath of the anaesthetic solution kept between 7 and 10 °C by an ice-water jacket.

Constant loads were applied to specimens and their extensions were measured through time using an apparatus similar to that diagrammed by Alexander (1962). Recovery tests, during which the loads were removed and decreases in specimen length were measured through time, were also conducted using that apparatus. The compliance (D, an index of extensibility) of a specimen was calculated,

$$D(t) = \frac{\Delta L(t)/L_0}{\sigma(t)},$$

where $\Delta L(t)$ is the change in length of the specimen at time t, and $\sigma(t)$ is the stress in the specimen at time t (calculated assuming the specimens were of constant volume). Specimens were submerged in anaesthetic; thymol was added to the anaesthetic of tissues tested for longer than 6 h to minimize bacterial decay of the specimens (there was no significant difference between the behaviour during the first several hours of extension tests of tissues in baths with and without thymol).

Mechanical testing of model tissues

The mechanical behaviour of a spiculated tissue must certainly depend upon the mechanical properties of the material in which the spicules are embedded as well as upon the nature of the attachment between this material and the spicules. In order to eliminate these two possible differences between tissues, models of spiculated tissues were constructed which all had the same type of material surrounding the spicules. Because spicule type and volume fraction in such models could be controlled, the models provided a system in which the mechanical effects of spicule size and shape, and of spicule packing density could be tested independently.

Spicules used in the models had been isolated from various animals. Fresh animal tissues were boiled in concentrated solutions of potassium hydroxide until they disintegrated. The spicules thereby released were cleaned by repeated rinsing in water and decanting, were then soaked for several weeks in a solution of sodium hypochlorite (10–14 %, w/v, available chlorine) to remove any remaining organic material, and were again repeatedly rinsed. Siliceous sponge spicules were then soaked in 1·5 % HCl for several weeks to eliminate any calcareous contaminants, and then repeatedly rinsed. Cleaned *Sarcophyton* spicules were sorted into two size classes by washing them through a 300 μm pore sieve, and *Dendronephthya* spicules were sorted into three size classes by passing them through first a 500 μm and then a 300 μm sieve. Some models were also prepared using reagent grade $CaCO_3$ powder as the 'spicules'.

Model tissues were prepared by embedding these spicules in gelatin. Spicules were weighed out into square dishes (22 × 22 mm) and equal volumes of melted gelatin (Maid Marian, raspberry) and of water were added to each to give spicule volume fractions of 0·01, 0·05, and 0·15 (and 0·32 when possible, i.e. when spicules had indices of packing (described below) greater than 0·32). These mixtures were gently heated by floating the dishes on hot water and were slowly stirred to remove air

bubbles and to evenly disperse the spicules. The dishes were then rapidly chilled on ice. The models were unmoulded, cut into strips, and kept in greased, covered Petri dishes until tested (within 24 h of their preparation). All specimens were visually inspected; only those specimens with evenly-dispersed spicules and no visible air bubbles or surface imperfections were used in mechanical tests.

Model tissues at room temperature were gripped and subjected to stress-extension tests as described above.

Morphology

Spicules for morphometric analysis were isolated as described above. In order to minimize sampling bias, vials containing spicules were inverted repeatedly before samples of spicules were removed for study. Some spicules were mounted in water on microscope slides; the length and width of spicules encountered along transects across the slides were measured to the nearest 10 μm using an eyepiece graticule in a compound microscope. Other spicules were mounted on stubs with double-sided cellophane tape, coated with gold (in a Polaron Equipment Ltd, SEM Coating Unit E5000) and photographed in a scanning electron microscope (Cambridge Stereoscan 600). Vernier callipers were used to measure the dimensions of various features of the spicules in such photographs. The surface areas and volumes of these spicules were calculated by modelling each spicule as a combination of cylinders, cones, hemispheres, and prolate spheroids. The 'index of packing', an estimate of the ability of spicules of various shapes to be packed together, was obtained by taking the ratio of the actual volume of spicules (calculated from their weight, using a density of 2·6 g.cm^{-3} for calcareous spicules (Jones, 1970) and of 2·2 g.cm^{-3}, the density of amorphous hydrated SiO_2 (Weast & Astle, 1978) for siliceous spicules) to the volume they occupied in a vial (measured to the nearest 0·01 cm^3) which had been tapped until the height of the spicules no longer changed with respect to marks on the vial.

The volume fraction of spicules in animal tissues was determined. The volume of a piece of tissue was ascertained by measuring with a pipette the volume of water displaced by the tissue when put into a filled volumetric flask. (Volume measurements were made three times and were repeatable to the nearest 0·01 cm^3.) The tissue was then blotted on filter paper and its wet weight was measured. (All weight mesaurements were made three times using a Mettler B6 balance and were repeatable to the nearest 0·001 g.) The specimen was then dried for 3 h in an oven at 110 °C and its dry weight measured. The tissue was then ashed in a muffle furnace at 500 °C for 3 h (see Paine, 1971) and the ash weight was measured. Known weights of sea water were also dried, ashed, and weighed. The volume fraction (γ) of spicules in a tissue was calculated,

$$\gamma = \frac{A_s}{\rho V},$$

where ρ is the density (g.cm^{-3}) of the spicules, V is the volume (cm^3) of the tissue, and A_s is the ash weight (g) due to the spicules,

$$A_s = A_T - \frac{A_w}{W_w}(W_s - D),$$

where A_T is the total ash weight (g) of the specimen, A_w is the ash weight of a given wet weight, W_w, of sea water, W_s is the wet weight of the specimen, and D is the dry weight of the specimen.

The structure of the tissues containing spicules was examined using S.E.M. Small blocks of tissue (which had been anaesthetized as described above) were fixed in 4% formaldehyde in sea water and prepared for S.E.M. using the procedure outlined by Mariscal (1974). Specimens were critical-point dried in CO_2, and then coated and photographed as described above.

The orientation of spicules in the cnidarians was measured. The angle (to the nearest 10°) between the longest axis of a spicule and the vertical axis of a colony was measured using a rotating eyepiece on a dissecting microscope for the first fifty spicules encountered in a tissue ($n = 3$ per species). Because the spicules in *A. digitatum* were smaller and more difficult to see than those of the other species, they were stained with alizarin red and the surrounding tissue was stained with Alcian blue and cleared with trypsin (Wassersug, 1976; Dinerkus & Uhler, 1977). The orientation of fibres seen in S.E.M.'s of *A. digitatum* coenenchyme was measured as described by Koehl (1977a).

Biologically relevant extensions and stresses in A. digitatum

The diurnal expansion and retraction of *A. digitatum* colonies was monitored. Seven colonies in aquaria at the Millport Marine Laboratory were photographed at timed intervals for 72 h. The ratio of the maximum height of an expanded colony to its minimum height when retracted should be equivalent to the longitudinal λ_{max} of the inner coenenchyme when the colony undergoes such a shape change. (The λ of the outer coenenchyme was difficult to measure accurately on the photographs because of the increase in diameter during colony expansion of the polyps perforating this tissue).

Drag forces (to the nearest 0·05 N) on *A. digitatum* colonies towed through sea water were measured using a Salter spring balance. Colonies were towed with their widest axis both perpendicular and parallel to the flow direction. The deflection of the tip of a calibrated plastic cantilever 1 cm long was used to measure the velocities (to the nearest 0·2 m.s^{-1}) at which colonies were towed. The projected areas of the colonies when orientated perpendicular and parallel to the flow direction were measured by tracing the colonies' perimeters on to mm^2 graph paper and counting the squares contained within the outlines; such tracings were made immediately after the drag measurements were taken. Stresses in each colony were calculated by assuming the colony was a cantilevered beam bearing the drag force as a load on its free end (see Koehl, 1977b).

RESULTS AND DISCUSSION
Morphology

The volume fractions of spicules in the types of tissues subjected to mechanical testing are listed in Table 1. Morphological features of the spicules used in the model tissues are listed in Table 2 and S.E.M.'s of these spicules are presented in Fig. 1. The orientations of spicules and fibres in the cnidarian tissues are presented in Fig. 3.
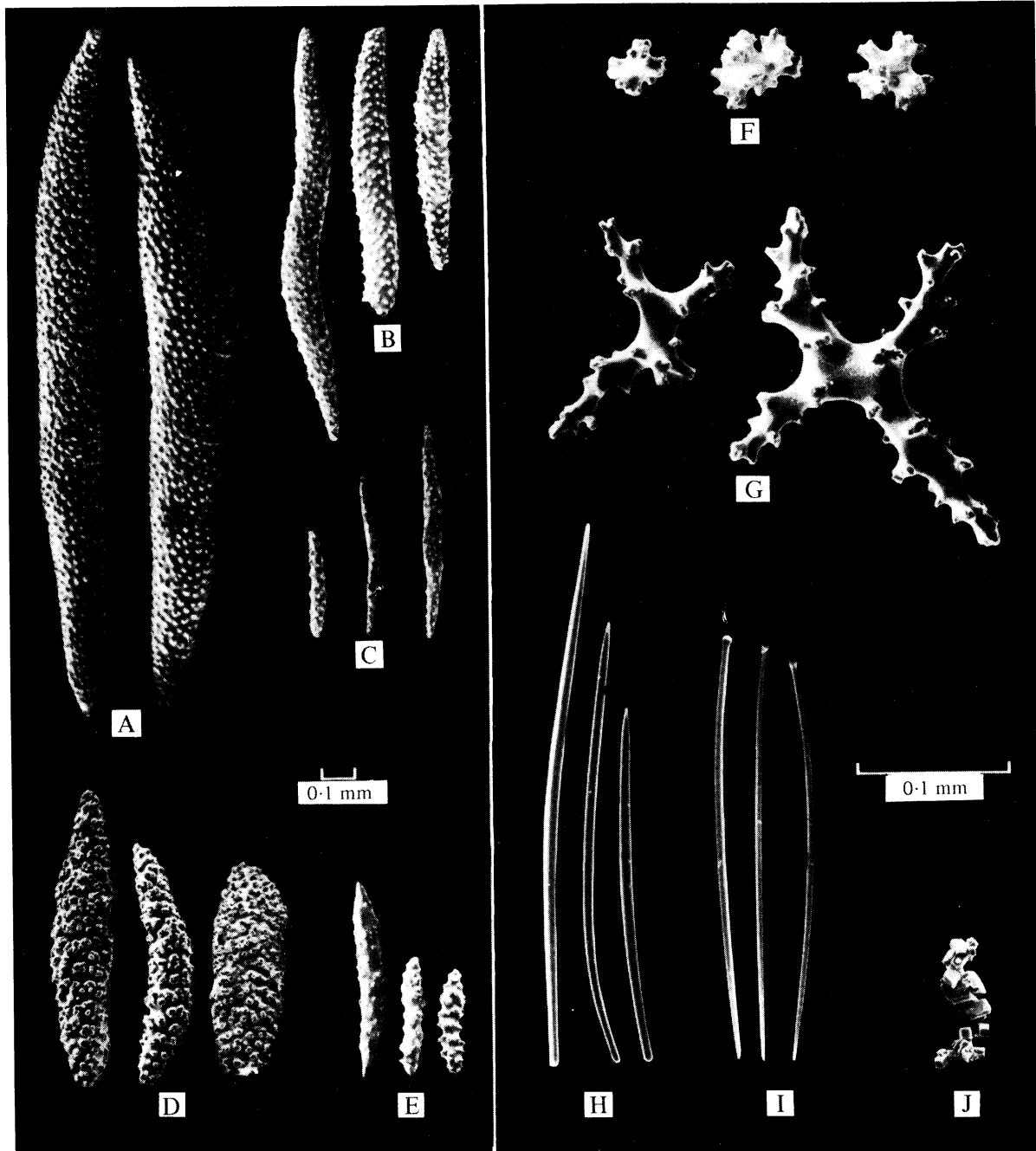
Fig. 1. SEMS's of spicules used in the model tissues. (A) *D. hemprichi*, large, (B) medium, and (C) small. (D) *S. glaucum* large, and (E) small. (F) *A. digitatum* outer, and (G) inner. (H) *H. sanguinea*. (I) *S. domuncula*. (J) $CaCO_3$ crystals.
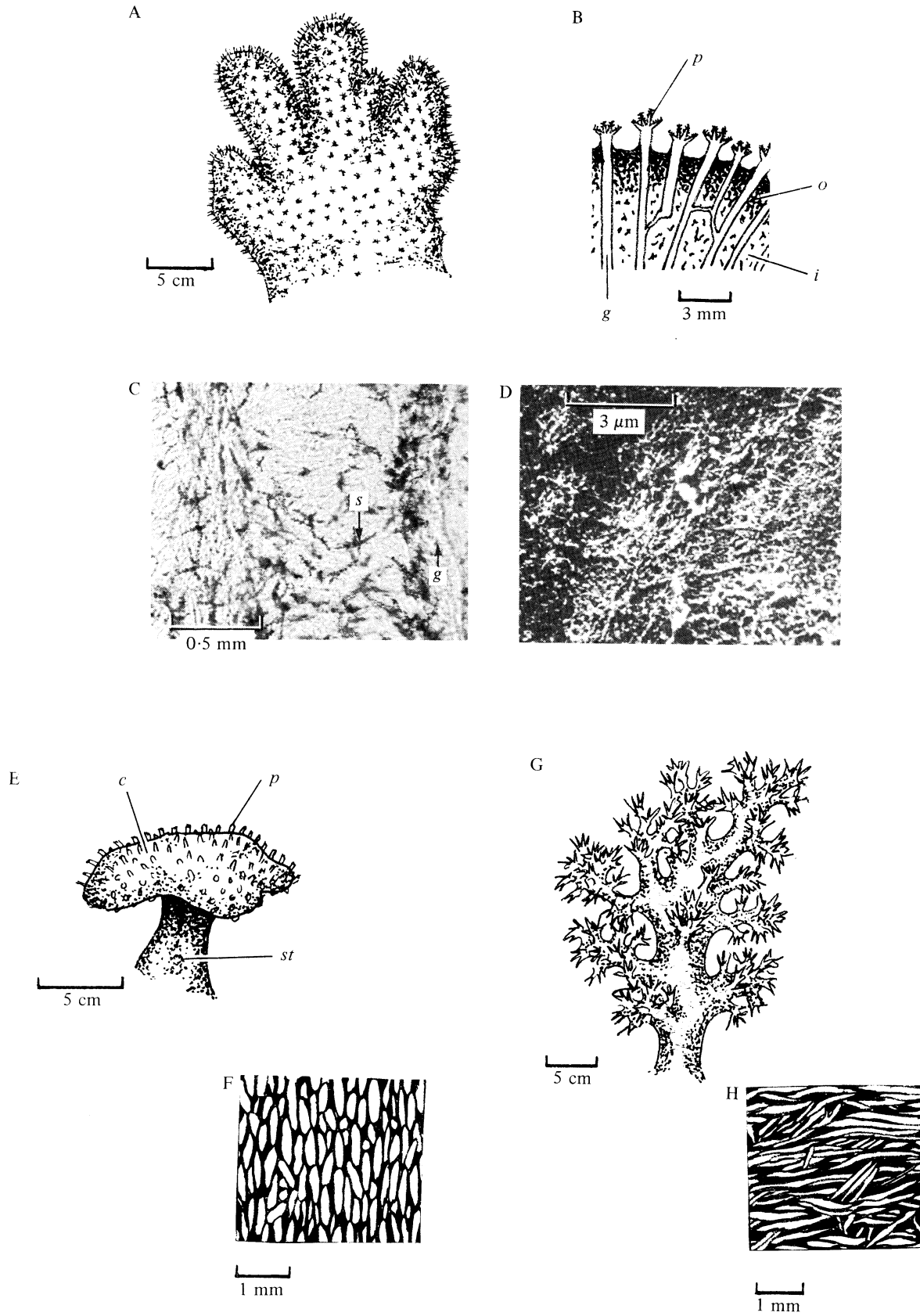
A

5 cm

B

p

o

i

g

3 mm

C

s

g

0·5 mm

D

3 µm

E

c

p

st

5 cm

F

1 mm

G

5 cm

H

1 mm

M. A. R. KOEHL

Table 2. *Spicule morphology*

Spicule type	Length (mm) ± s.d. (n = 82)	Length/width ± s.d. (n = 12)	Surface area/ volume (mm²/mm³) ± s.d. (n = 3)	Index of packing ± s.d. (n = 2)
A. digitatum, outer	0·07 ± 0·03	1·3 ± 0·3	787 ± 170	0·25 ± 0
A. digitatum, inner	0·21 ± 0·09	5·0 ± 1·4	227 ± 47	0·22 ± 0·01
D. hemprichi, large	1·72 ± 0·45	9·5 ± 2·8	17 ± 2	0·28 ± 0·01
D. hemprichi, medium	1·23 ± 0·36	8·7 ± 3·5	35 ± 2	0·25 ± 0·06
D. hemprichi, small	0·20 ± 0·09	10·0 ± 2·8	78 ± 24	0·32 ± 0·03
S. glaucum, large	0·90 ± 0·15	4·4 ± 0·7	33 ± 7	0·32 ± 0·06
S. glaucum, small	0·34 ± 0·18	7·4 ± 2·8	105 ± 50	0·34 ± 0
$CaCO_3$ crystals	0·05 ± 0·03*	1·7 ± 0·7*	642 ± 153*	0·34 ± 0·03
S. domuncula	0·23 ± 0·09	49·8 ± 11·8	762 ± 143	0·15 ± 0
H. sanguinea	0·32 ± 0·09	48·8 ± 11·1	472 ± 54	0·06 ± 0·01

* $CaCO_3$ crystals tended to form clumps (Fig. 1F). These measurements were made on clumps rather than individual crystals. Surface area was estimated assuming individual crystals to be cubes with half of their surface area exposed when in a clump.

The fleshy colonies of the soft coral *A. digitatum*, 'dead man's fingers' (Fig. 2A and B), are composed of connective tissue (coenenchyme) penetrated by the cylindrical gastrovascular cavities of the polyps and some fine strands of cells (see Hickson, 1895, 1901). The coenenchyme near the surface of the colony (to which I will refer as 'outer coenenchyme') contains small (Fig. 1F) closely-packed spicules. In contrast, the 'inner coenenchyme' contains larger (Fig. 1G), more dispersed (Fig. 2C) spicules. The coenenchyme of *A. digitatum* is fibrous (Fig. 2D) and the fibres appear to be in intimate association with the spicules, although the nature of the attachment, if any, of the fibres to the spicules has not yet been worked out. The longest arms of spicules of the inner coenenchyme tend to be orientated at low angles with respect to the vertical axis of the colony (Fig. 3A), whereas the fibres do not show any preferred orientation (Fig. 3B). The connective tissue of the coenenchyme stains with Alcian blue, which is specific for mucopolysaccharides (Dingerkus & Uhler, 1977). If this tissue is similar in composition to the cnidarian connective tissues that have been more extensively analysed (for a review, see Koehl, 1977a), it is composed of collagen fibres in a amorphous mucopolysaccharide matrix.

Fig. 2. Alcyonaceans whose spiculated connective tissues were used for mechanical testing. All colonies and sections of tissues shown have their vertical axis parallel to the vertical axis of the page. (A) Diagram of a colony of *A. digitatum*. (B) Diagram of a longitudinal section through the tip of a branch of an *A. digitatum*. The gastrovascular cavities (g) of the polyps (p) extend into the fleshy coenenchyme. The spicules, which are indicated by dark spots, are more densely packed in the outer coenenchyme (o) than in the inner coenenchyme (i). (C) Micrograph of a longitudinal section (1 mm thick) of the inner coenenchyme of a cleared *A. digitatum* with stained spicules (s). The gastrovascular cavity (g) of a polyp is shown. (D) SEM of the connective tissue in between the spicules of the inner coenenchyme of an *A. digitatum*. Note the feltwork of fibres in the tissue. (E) Diagram of a colony of *S. glaucum*, showing the polyp (p) -covered capitulum (c) supported on the stalk (st). (F) Diagram of a longitudinal section through the stalk of a *S. glaucum*. The spicules are shown as white and the surrounding connective tissue as black. (G) Diagram of a colony of *D. hemprichi*. The stalk and branches of the colony are hollow, thin-walled, and hydrostatically supported. (H) Diagram of a surface view of the stalk wall of a *D. hemprichi*. The spicules are shown as white and the surrounding connective tissue as black.

M. A. R. KOEHL

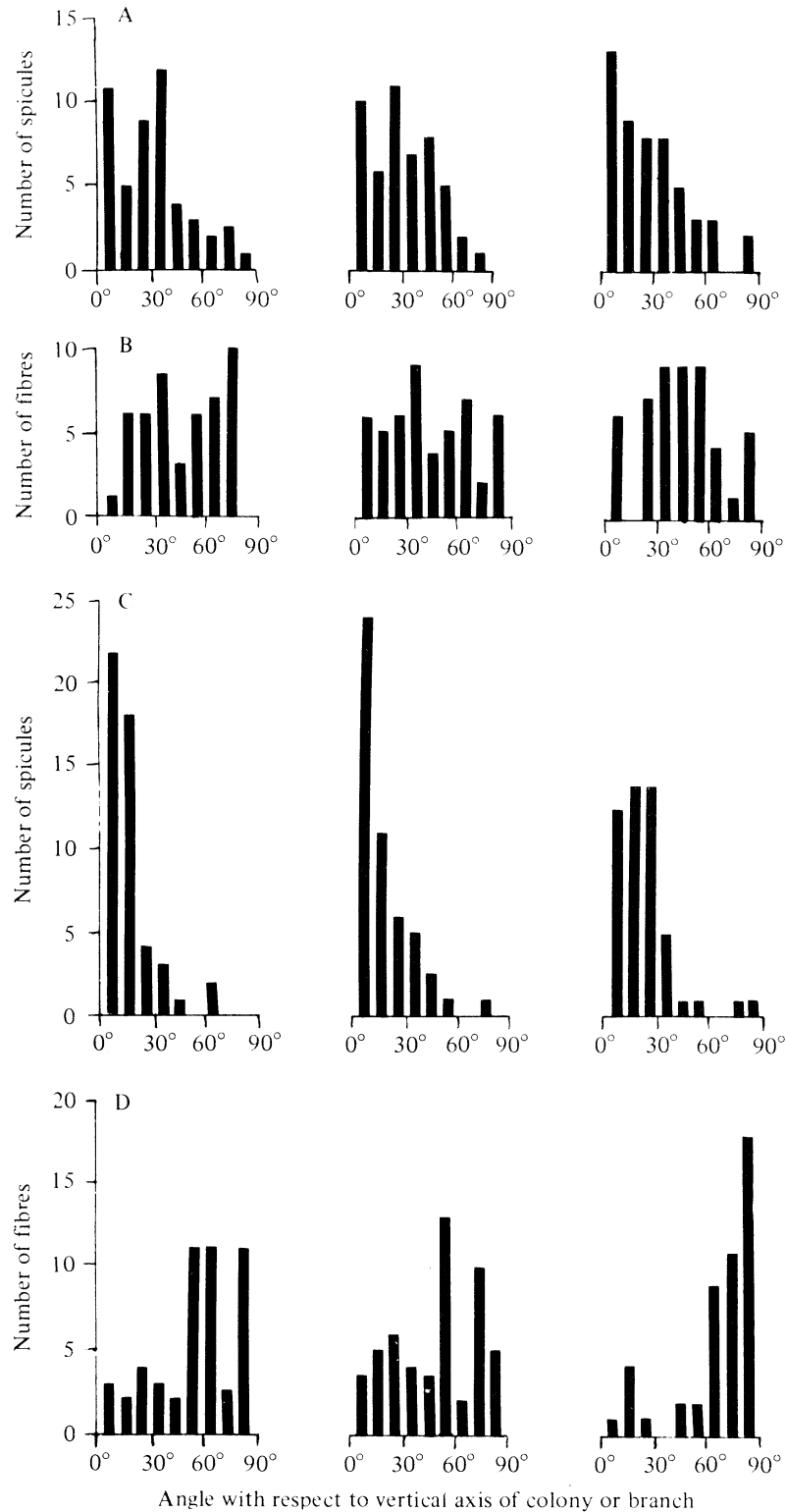Angle with respect to vertical axis of colony or branch

Fig. 3. Histograms of orientations of (A) spicules in *A. digitatum* inner coenenchyme, (B) fibres in *A. digitatum* inner coenenchyme, (C) spicules in *S. glaucum* stalk, and (D) spicules in *D. hemprichi* branch wall. Each histogram represents a separate specimen.
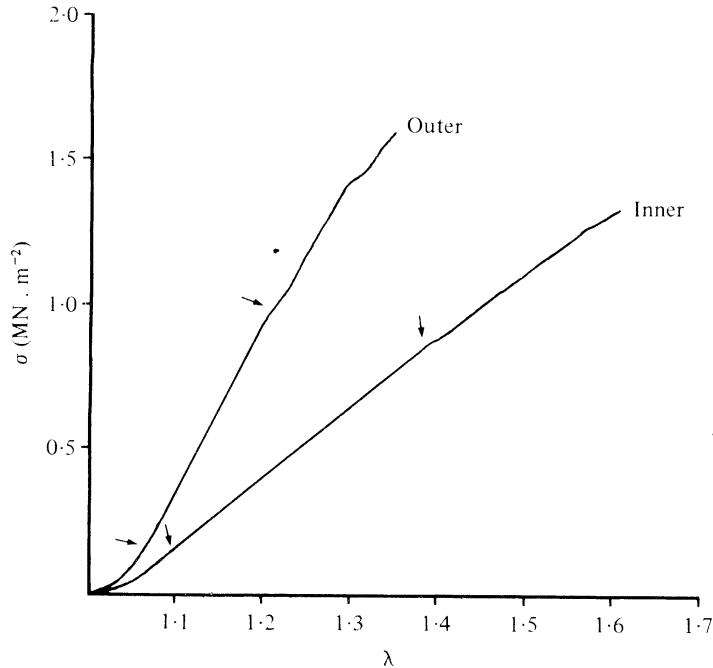
Fig. 4. Stress (σ) – extension (λ) curves for inner and outer coenenchyme of *A. digitatum* pulled at $\dot{\epsilon} = 0.04$ s^{-1}. The portions of the curves between the arrows were used to calculate E. The curves end where the specimens broke.

Colonies of the soft coral *Sarcophyton glaucum* are mushroom-shaped, with a broad, polyp-covered capitulum supported on a stalk (Fig. 2 E). The stalk contains large (Fig. 1 D, E), closely-packed spicules which tend to be orientated at low angles with respect to the vertical axis of the stalk (Figs. 2 F and 3 C).

The tree-like branching colonies of the soft coral *Dendronephtya hemprichi* are hydrostatically supported. The cylindrical branches (Fig. 2 G) of these colonies are composed of a layer of spiculated connective tissue (one spicule layer thick) surrounding a fluid-filled space. The large spicules (Fig. 1 A, B) in the connective tissue tend to be orientated at large angles with respect to the longitudinal axis of a branch (Figs. 2 H and 3 D). The small spicules (Fig. 1 C) isolated from this species are found in the polyps.

Mechanical properties of spiculated connective tissues

In the following section the behaviour of spiculated tissues when subjected to various mechanical tests will be described and compared to the behaviour of filled polymers. The mechanics of filled polymers, which will only be briefly summarized here, is described in much greater depth in articles and reviews such as those by Christensen (1979), Dickie (1977), Farris (1972), Fedors & Landel (1975), Ferry (1970), Kotani & Sternstein (1972), Kraus (1965), Lepie & Adicoff (1972), Mark (1970), Mascia (1974), Mullins (1963, 1980), Titow & Lanham (1975) and Wake (1971).

Stiffness

Typical stress–extension curves for the lightly spiculated inner coenenchyme and the heavily spiculated outer coenenchyme of *A. digitatum* are shown in Fig. 4. The
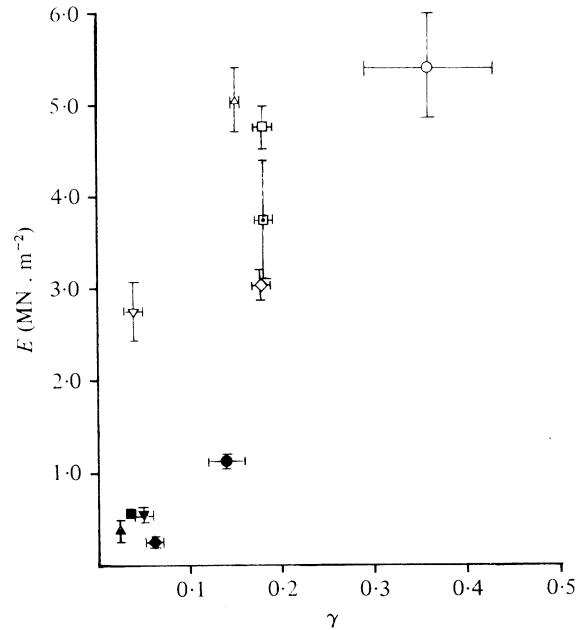
Fig. 5. Modulus of elasticity (E) of tissues containing different volume fractions (γ) of spicules pulled at $\dot{\epsilon} = 0.04\ \mathrm{s}^{-1}$. Open symbols indicate mean values for cnidarian tissues: *S. glaucum* stalk (○), *A. digitatum* outer coenenchyme (△) and inner coenenchyme (▽), and *D. hemprichi* mid-branch wall (with circumferentially orientated spicules; see Fig. 3) pulled circumferentially (□) and longitudinally (◇), and *D. hemprichi* wall from branch bifurcations (with randomly orientated spicules) (⊡). The E of large-spiculed *D. hemprichi* tissue is lower than that of *A. digitatum* inner coenenchyme, although the ranges of γ's of these two types of tissue overlap. If the magnitude of γ for these two types of tissue is considered to be the same, then the E and γ of cnidarian tissues are significantly directly associated (Kendall Tau: $T = 0.91$, $n = 4$, $P = 0.05$ (Gibbons, 1976)). The E of *S. glaucum* mid-branch tissue pulled circumferentially is significantly larger than that of this tissue pulled longitudinally (ANOVA: $F_{[1,6]} = 10.8$, $0.01 < P < 0.025$ (Sokal & Rohlf, 1969)). Closed symbols indicate mean values for sponge tissues: *S. domuncula* (●), *S. ciliatum* (▲), *H. panicea* (■), *H. sanguinea* (▼), and *G. compressa* (◆). The E's of *S. ciliatum*, *H. panicea*, *H. sanguinea*, and *G. compressa* were not significantly different and were pooled; the E of these lightly-spiculated sponges was significantly lower than that of the more heavily spiculated *S. domuncula* (ANOVA: $F_{[1,14]} = 50.5$, $P < 0.001$). Error bars indicate one standard error.

portion of each curve used to calculate the elastic modulus (E) is indicated between the arrows. Note that the curve is steeper (E is higher) for the heavily spiculated tissue.

In Fig. 5 the E's of tissues from various species of cnidarians and sponges are plotted against the volume fraction of spicules in such tissues. These results suggest that spicules stiffen tissues. For example, the tissues from alcyonaceans with high spicule contents tend to be stiffer than those with low spicule contents. The E's of these spiculated cnidarian tissues are about ten times greater than those of un-spiculated sea anemone mesogloea (Alexander, 1962; Gosline, 1971; Koehl, 1977a, b) and are of the same order of magnitude as those of zoanthid body walls reinforded with sand grains and spicules (Koehl, 1977c). Similarly, tissues from the sponge *Suberites domuncula* are significantly stiffer than those of the more lightly spiculated sponges tested (Fig. 5). (That the cnidarian tissues have higher E's than the sponge tissues could be due to differences in the stiffness of the material between the spicules, to differences in the adhesion of spicules to this material, and/or to the fact that sponges are riddled with microscopic holes which were not subtracted from the cross-sectional areas of the specimens when the E's were calculated.)

Many pliable connective tissues of animals, such as the mesogloea of cnidarians (Koehl, 1977a) and the mesohyl of sponges (Garrone, Huc & Junqua, 1975; Junqua, Fayolle & Robert, 1975; Berquist, 1978) are composed of collagen fibres dispersed in an amorphous matrix of highly hydrated mucopolysaccharide polymers. When such a tissue deforms in response to a load, collagen fibres that are folded straighten out, and the fibres may be reorientated and/or slide relative to each other as the polymer molecules in the matrix rearrange (Viidik, 1972; Wainwright *et al.* 1976). The mechanical behaviour of the amorphous matrix of such tissues has been likened to that of other pliable polymeric materials (see Ferry, 1970). At low extensions the coiled molecules of the matrix rearrange locally and straighten out, offering little resistance to deformation. At greater extensions, further molecular rearrangement is hindered by entanglements and the material offers more resistance to deformation. At still larger extensions, the material will continue to flow by entanglement slippage unless the polymer molecules are cross-linked together to form a network. If one pulls such a network to extensions where the cross-links prevent further rearrangement of molecules, one is pulling on the 'backbones' of some of the molecules and the material is stiff; further extension can only occur if molecules and/or cross-links break to allow rearrangement.

When rigid particles (such as spicules or carbon black) are embedded in a deformable material (such as mesogloea or rubber), the resulting composite is stiffer than the deformable material on its own. Such rigid 'filler' particles take up space and thereby restrict the motion of the polymer molecules around them, hence fillers hinder the rearrangement of those molecules in response to a load. Furthermore, when a filled polymer is deformed, the rigid space-occupying inclusions do not change shape, but may translate and/or rotate relative to each other; local deformations of the pliable polymer between the filler particles, therefore, can be much greater than the overall deformation of the composite. These effects of restricting molecular rearrangement in response to a stress, and of local strain amplification, are more pronounced if the filler particles are cross-linked to the polymer molecules. Since fillers increase the stiffness of polymers by taking up space, and in some cases by adding cross-links to the polymer network, the greater the volume fraction of filler in a deformable material, the stiffer the composite will be. It is not surprising, therefore, that those animal tissues containing a greater volume fraction of spicules have higher E's than similar tissues with fewer spicules.

Stress-softening

Typical results of cyclic stress–extension tests of the heavily spiculated outer co-enenchyme from *A. digitatum* are shown in Fig. 6A. Note that the stress–extension curves for each successive pull of a specimen of outer coenenchyme follow the retraction curves of the previous cycle. The stress required to extend a specimen a given amount is greater during the first pull than during subsequent pulls to extension ratios smaller than the maximum extension ratio of the first pull (compare circles in Fig. 6). Similarly, the extension ratio achieved for a given application of stress is greater on subsequent pulls (compare stars in Fig. 6). The area under a stress–extension ratio curve is the work per volume required to extend the tissue; less work is required to pull a tissue to a given λ on subsequent pulls than on the first pull.
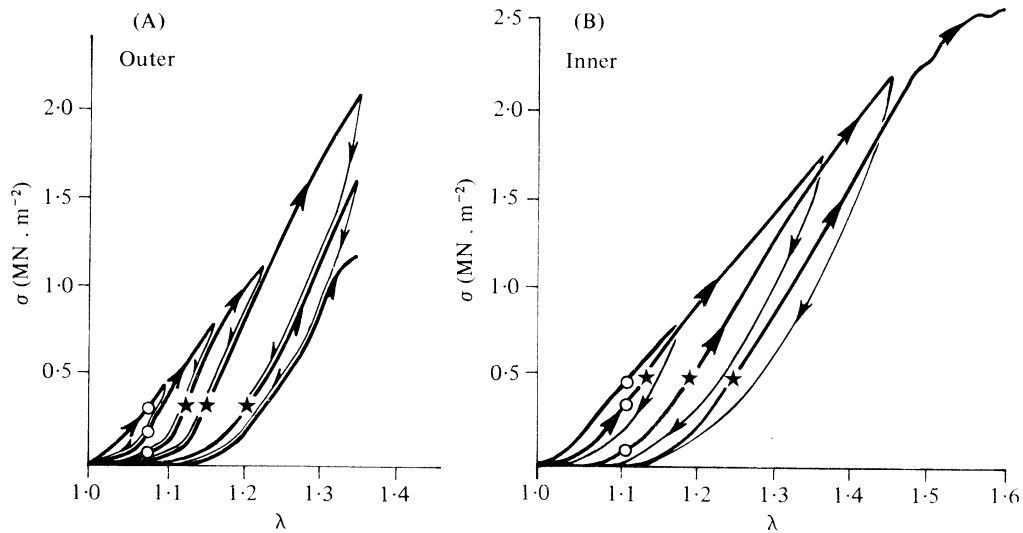
Fig. 6. Stress (σ) – extension (λ) curves for strips of *A. digitatum* coenenchyme subjected to cyclic tests ($\dot{\epsilon} = $ 0·04 s^{-1}) until they broke. Tissues were being pulled when arrows point upwards and to the right and were being returned to their original length when arrows point downwards and to the left. (A) Outer coenenchyme (results typical of 9 such tests run). (B) Inner coenenchyme (results typical of 5 such tests run). Stars and circles are explained in the text.

The behaviour of outer coenenchyme when subjected to cyclic stress–extension tests is known as 'stress softening' (the 'Mullins effect') and is characteristic of filled polymers. Various models have been proposed to explain this phenomenon (see references about filled polymers cited above). A basic feature of most of these models is that, because local strains in filled polymers can be quite high, local 'failures' (such as permanent slippage or breakage of polymer chains, or formation of voids between filler particles and the polymer) can occur at low extensions of the composite. On subsequent pulls these chains or attachments no longer contribute to resisting the deformation of the material, which therefore extends more easily. The slope of the stress–extension ratio curve of such a 'softened' material is low until it is pulled to extensions where molecules which were maximally extended, but not broken (or detached, or slipped), on previous pulls again are maximally extended and therefore offering a great deal of resistance to further stretching of the composite. At such λ's the slope of the stress–extension curve ratio shows a marked increase (Fig. 6A). At λ's greater than that of previous pulls, the slope of the stress–extension curve is the same as it would be if the material had not been previously pulled. Typical results of cyclic stress–extension tests of the lightly spiculated inner coenchyme of *A. digitatum* are given in Fig. 6B. The stress-softening behaviour described above is less pronounced in this material, as would be expected for a tissue containing fewer spicules and therefore subjected to less local strain-amplification.

Both outer and inner coenenchyme often failed at lower stresses than those achieved on earlier pulls (9 of the 21 specimens of outer coenenchyme; 6 of the 21 specimens of inner coenenchyme). Such behaviour is consistent with the hypothesis that stress-softening in these tissues is due to local failures within the tissues.
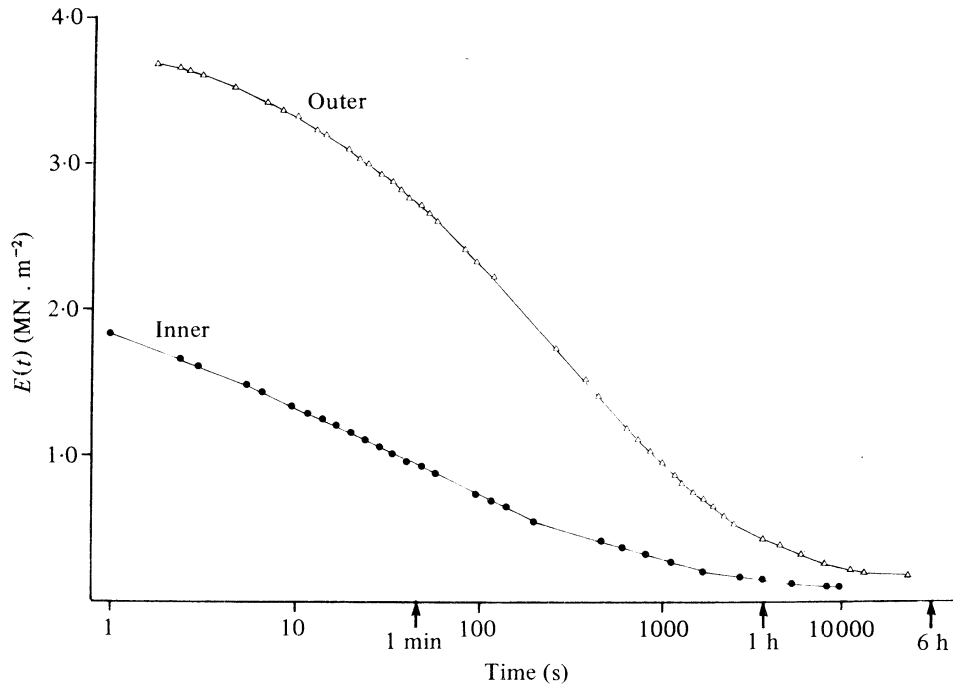
Fig. 7. Time-dependent modulus ($E(t)$) plotted against time, on a logarithmic scale, for inner
(●) and outer (△) coenenchyme from an *A. digitatum* colony. Each tissue was extended to
$\lambda = 1\cdot20$ at the beginning of the test. Three long-term and fifteen short-term stress–relaxation
tests were conducted on inner coenenchyme, and two long-term and eighteen short-term tests
were conducted on outer coenenchyme.

Time-dependent mechanical behaviour

Results of stress–relaxation tests of inner and outer coenenchyme of *A. digitatum*
are shown in Fig. 7. Although the heavily spiculated outer coenenchyme is stiffer than
the lightly-spiculated inner coenenchyme just after the tissues have been extended,
the modulus of the outer tissue decreases more than that of the inner tissue when the
tissues are held at a given extension for several hours.

Results of extension at constant load tests on inner and outer coenenchyme are
shown in Fig. 8. When these tissues are subjected to a constant load for several hours,
the compliance of the heavily spiculated outer tissue increases more than does that
of the lightly spiculated inner tissue.

Filled polymers exhibit 'time-dependent Mullins effect'; the greater the volume
fraction of filler in a polymer, the more pronounced the time-dependent softening. It
can be postulated that similar sorts of microfailures and rearrangements within the
material that are responsible for the stress-softening described above are also re-
sponsible for the time-dependent stress–relaxation and creep of these materials
(Farris, 1972). The observations that spiculated coenenchyme sometimes breaks while
relaxing (two specimens of outer coenenchyme at λ's of $1\cdot49$ and $1\cdot61$, and one
specimen of inner coenenchyme at a λ of $1\cdot34$), and that it does not return to its
original length during creep-recovery tests (Fig. 9) are consistent with the hypothesis
that some of the time-dependent softening of this material is due to microfailures in
the tissue. In contrast, the unspiculated mesoglea of sea anemones does slowly return
to its resting length during recovery tests (Alexander, 1962; Koehl, 1977a).
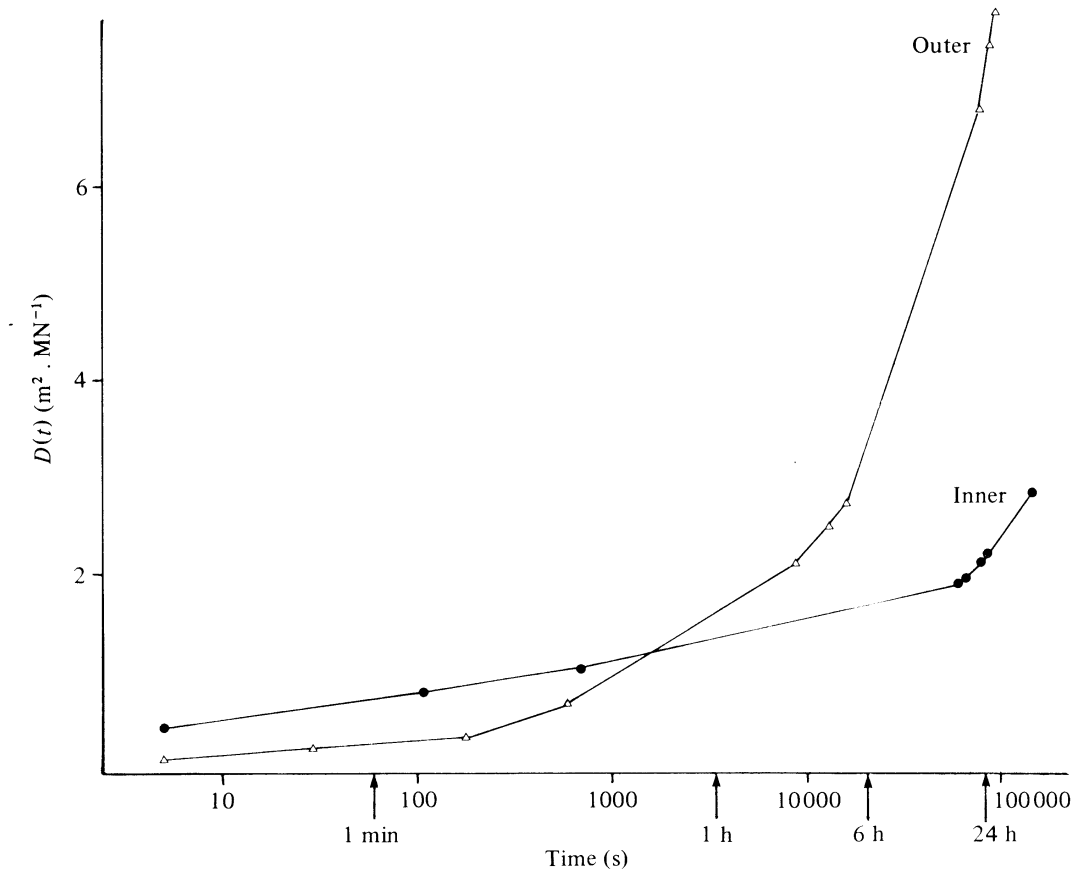
Fig. 8. Compliance ($D(t)$) plotted against time, on a logarithmic scale, for inner (●) and outer (△) *A. digitatum* coenenchyme subjected to constant loads. These two specimens were taken from one colony. The initial stress in the inner tissue was 0.11 $MN.m^{-2}$, and in the outer tissue was 0.06 $MN.m^{-2}$. Sixteen such tests were run on outer coenenchyme, and seven were run on inner coenenchyme.
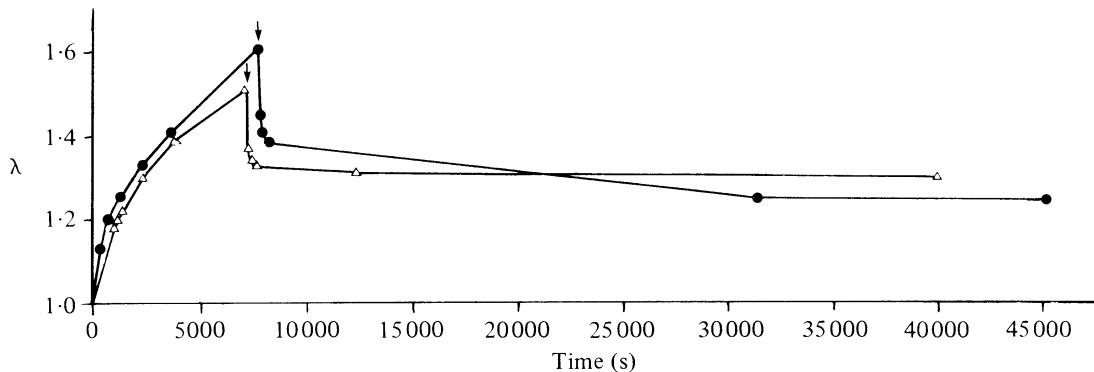

Fig. 9. Extension under constant load and recovery curves (λ vs. time) for inner (●) and outer (△) coenenchyme from an *A. digitatum*. An arrow indicates the point when the weight was removed from a specimen. The initial stress in the inner tissue was 0.20 $mn.m^{-2}$, and in the outer tissue was 0.31 $MN.m^{-2}$. During recovery periods equal to the time during which the load had been applied, inner coenenchyme shortened by only 45% (S.D. $= 4.2$, $n = 4$) and outer coenenchyme shortened by only 48% (S.D. $= 11.6$, $n = 4$) of the amount they had stretched. Even two tissues allowed to recover for longer than 19 h did not return to their original length.
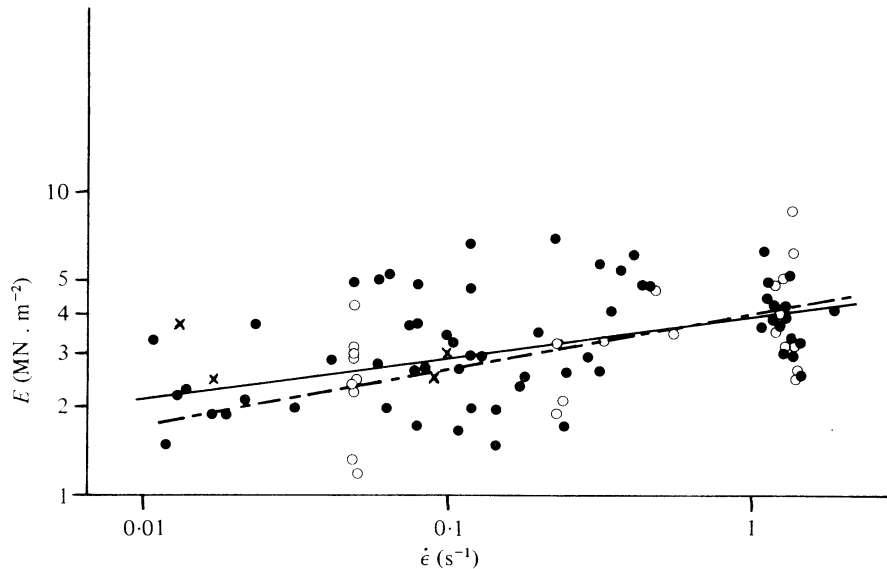
Fig. 10. Graph of elastic modulus (E) on a logarithmic scale against strain rate ($\dot{e}$) on a logarithmic scale for *A. digitatum* inner coenenchyme. The x's indicate data points for un-anaesthetized specimens pulled longitudinally. The dashed line represents the regression line fitted by the least squares method (Sokal & Rohlf, 1968) to the set of data points for anaesthetized specimens pulled transversely ($\bigcirc$), and the solid line represents the regression line fitted to the data points for anaesthetized specimens pulled longitudinally ($\bullet$). These regression lines are not significantly different from each other in slope (ANCOVA: $F_{1,82} = 1\cdot48$, $0\cdot10 < P < 0\cdot25$ (Snedecor, 1956)) or elevation ($F_{1,83} = 1\cdot79$, $0\cdot10 < P < 0\cdot25$). By pooling the data for all anaesthetized specimens, the relationship between modulus and extension rate for *A. digitatum* inner coenenchyme is found to be $E = 3\cdot97 \; (\dot{e})^{0\cdot13}$.

Strain-rate-dependent stiffness

The E's of *A. digitatum* inner and outer coenenchyme pulled at different rates are plotted in Figs. 10 and 11 respectively. Anthozoan mesogloea has been found to be a viscoelastic material (Alexander, 1962; Gosline, 1971; Koehl, 1977 a, b), hence the more rapidly it is pulled, the stiffer it is. If filler particles are put into polymeric materials whose resistance to deformation is independent of strain rate, the composite exhibits 'shear-thinning' behaviour: the more slowly the material is deformed, the stiffer it will be (Nicodemo & Nicolais, 1974 a, b; Nicodemo, Nicolas & Landel, 1974). Hence it might be expected that if fillers (spicules) are contained in a material such as mesogloea that exhibits viscoelastic behaviour (i.e. the more slowly the material is deformed, the less stiff it will be) the viscoelastic strain-rate dependence of the composite should be reduced, cancelled, or reversed as spicule content increases. It is not surprising, therefore, that the E of the heavily spiculated outer coenenchyme is nearly strain-rate-independent (Fig. 11) while the E of the lightly-spiculated inner coenenchyme increases slightly with strain rate (Fig. 10). As expected, the E of unspiculated mesogloea from sea anemones increases more with strain rate (Koehl, 1977 b) than does that of spiculated inner coenenchyme.

Note that the unanesthetized pieces of outer coenenchyme (X's in Fig. 11) have much higher E's than anaesthetized specimens. That unanaesthetized pieces of the more sparsely muscled (Hickson, 1895, 1901) inner coenenchyme (X's in Fig. 10) are less stiff than unanaesthetized outer tissue and are of similar stiffness to anaesthetized
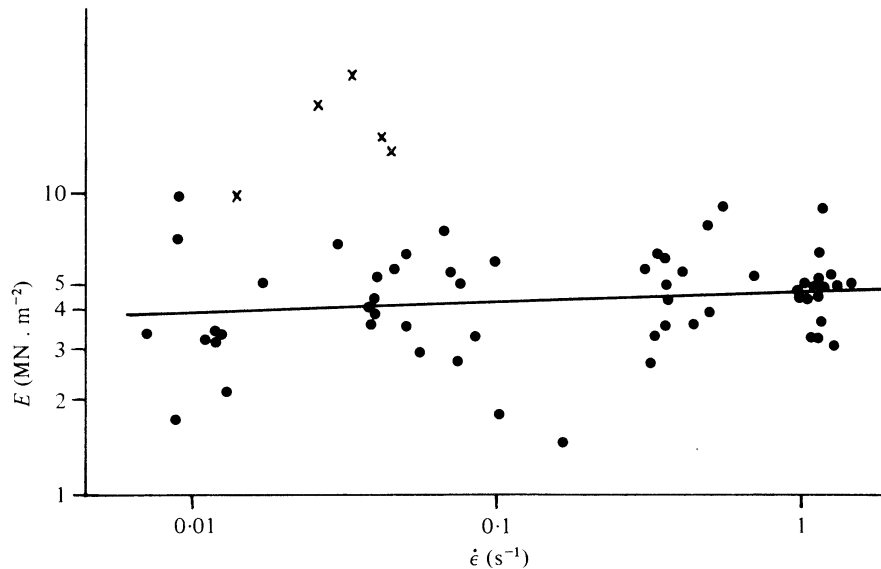
M. A. R. KOEHL

Fig. 11. Graph of elastic modulus (E) on a logarithmic scale against strain rate ($\dot{e}$) on a logarithmic scale for *A. digitatum* outer coenenchyme. The line represents the regression line fitted to the set of data points for anaesthetized specimens. This line for outer coenenchyme is significantly different in slope from that for inner coenenchyme (Fig. 10) (ANCOVA: $F_{1,142} = 6.06$, $0.01 < P < 0.025$). The relationship between modulus and strain rate for *A. digitatum* outer coenenchyme is found to be $E = 4.78\ (\dot{e})^{0.04}$. The x's indicate data points for unanaesthetized specimens.

inner coenenchyme suggests that contracting muscles are responsible for the higher E's of unanaesthetized outer coenenchyme. These observations should serve as reminders that many animals can actively control their stiffness by contracting muscles.

Isotopy or aniostropy of mechanical behaviour

The stiffness of a composite material composed of a pliable matrix containing long or continuous fibres, which bear in tension part of the load on the material, depends upon the orientation of the fibres with respect to the axis along which the material is pulled:

$$E \propto \Sigma\ a_n \cos\ ^4\phi,$$

where a_n is the proportion of fibres in a plane at angle ϕ to the stress axis (Wainwright *et al.* 1976). Furthermore, the deformation of the matrix in a material reinforced with elongate filler particles or short fibres is greatest for a given overall extension of the composite if it is pulled along axes parallel to the particles or fibres, hence such a material is stiffest along these axes (Gosline, 1971; Wainwright *et al.* 1976). Therefore, one would expect animal tissues having an anisometric arrangement of fibres and/or spicules to be mechanically anisotropic. A number of pliable biological materials reinforced with fibres showing a preferred orientation have been found to be stiffest when pulled parallel to the fibres (Wainwright *et al.* 1976); one such material is the mesogloea of sea anemones (Gosline, 1971; Koehl, 1977*a*).

The colonies of *D. hemprichi* and *A. digitatum* were wide enough that samples could be cut from them for transverse as well as longitudinal stress-extension testing. *D. hemprichi* coenenchyme is significantly stiffer when pulled circumferentially than when pulled longitudinally (Fig. 5). The long spicules in this coenenchyme tend to be

orientated at high angles with respect to the long axis of the colony (Fig. 3 D). In contrast, inner coenenchyme from *A. digitatum* is not significantly stiffer when pulled longitudinally than when pulled circumferentially (Fig. 10). The fibres of this tissue are arranged in a feltwork (Fig. 2 D) and do not show a preferred orientation (Fig. 3 A). Although the spicules show a slight tendency to be orientated with their longest arms at small angles to the longitudinal axis of the colony (Fig. 3 A), the spicules are short and only slightly-anisometric in shape (Table 2).

Mechanical behaviour of model tissues

That the gelatine 'tissues' are reasonable models of cnidarian tissues is illustrated in Fig. 12. The stress–extension curves plotted up to the yield point for cnidarian connective tissue without spicules (*M. senile* mesogloea) and with 0·15 volume fraction of spicules (*A. digitatum* outer coenenchyme) are presented in Fig. 12 A. Stress–extension curves for gelatin tissue without spicules and with 0·15 volume fraction of spicules (isolated from *A. digitatum* outer coenenchyme) are presented in Fig. 12 B. Note that, although the model tissues are about one tenth as stiff as the real tissues, the yield extensions of the models and real tissues are comparable, as are the stiffening effects of the spicules.

Volume fraction of spicules

The moduli of models containing different volume fractions of particular types of spicules are plotted in Fig. 13. Of the models containing 0·01 and 0·05 volume fraction of spicules, only those containing sponge spicules or $CaCO_3$ crystals are significantly stiffer than unspiculated models. All models containing 0·15 (and 0·32 in the two cases possible) volume fraction spicules, however, are significantly stiffer than the unspiculated gelatin. The results plotted in Fig. 13 indicate that (1) the greater the volume fraction of spicules, the stiffer the tissue, and (2) some types of spicules are more stiffening than others.

The moduli of various model tissues pulled at different strain rates are plotted in Fig. 14. Note that the models either exhibit strain-rate-independent behaviour or are stiffer when pulled slowly than when pulled quickly. Note again that models containing high volume fractions of spicules are stiffer than those with lower spicule contents.

Aspect ratio of spicules

The monaxon sponge spicules, which have a much greater stiffening effect than the other spicules tested, have a very high aspect ratio (length/diameter) compared with the other spicules. There is no correlation, however, between the aspect ratios of the other spicules and the *E*'s of the models they reinforce (Fig. 15).

If a composite composed of discontinuous stiff fibres or rods in a pliable matrix is pulled, tensile stresses in the matrix are transmitted to the fibres via shear stresses at the fibre-matrix interfaces. The length at each end of a fibre over which stresses are transferred (i.e. shear stresses at the matrix-fibre interface decrease and tensile stresses in the fibre increase to some maximum value) is the 'transfer length' (l_T),
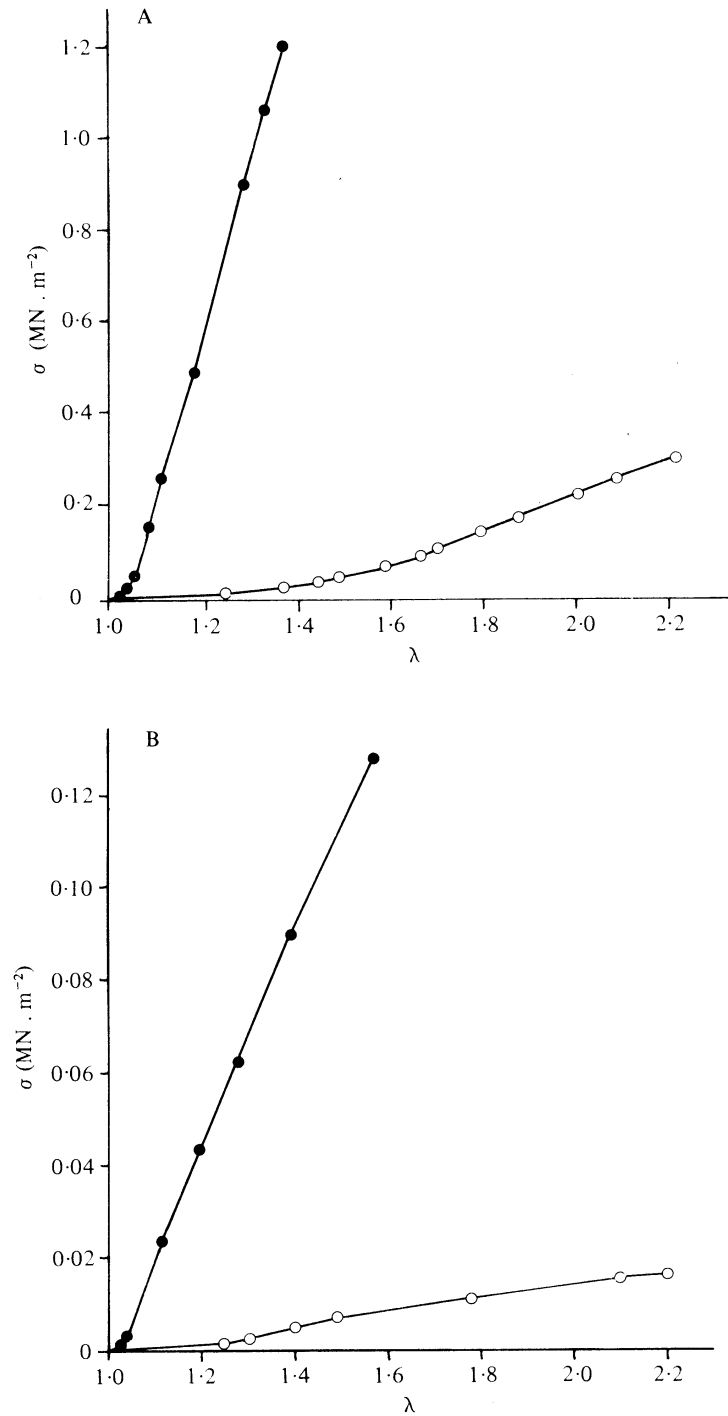
$$l_T = r\sigma_F/\tau,$$

Fig. 12. Stress (σ) – extension (λ) curves for unspiculated ($\bigcirc$) and spiculated ($\bullet$) specimens of (A) cnidarian connective tissue: *Metridium senile* (sea anemone) mesoglea ($\bigcirc$), and *A. digitatum* outer coenenchyme ($\bullet$), and (B) model 'tissues': gelatine ($\bigcirc$), and gelatine containing spicules ($\gamma = 0.15$) from *A. digitatum* outer coenenchyme ($\bullet$). Specimens were pulled at $\dot{\epsilon} = 0.04$ s^{-1} until they broke.
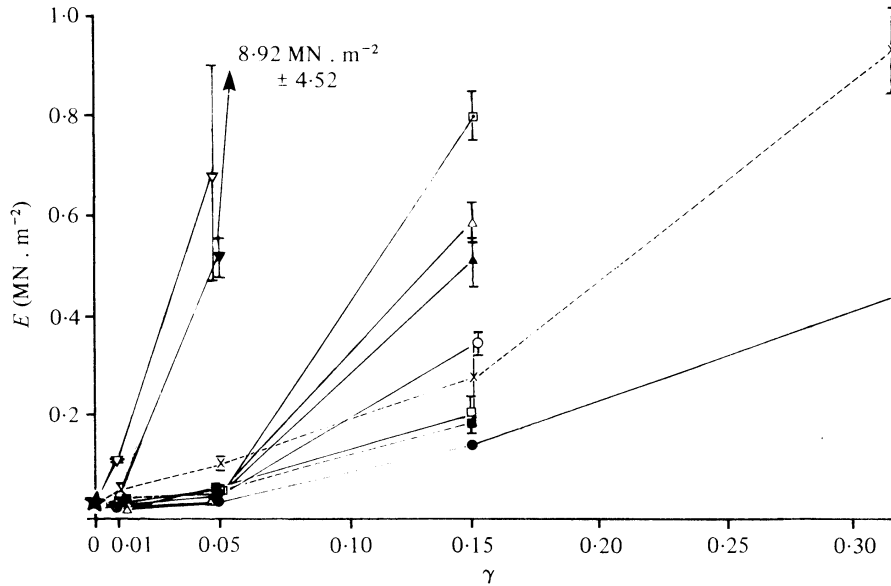
Fig. 13. Graph of the mean moduli of elasticity (E) of model 'tissues' containing different volume fractions (γ) of spicules: the cnidarian spicules *A. digitatum* inner ($\triangle$) and outer ($\blacktriangle$), *S. glaucum* small ($\bigcirc$) and large ($\bullet$), and *D. hemprichi* small ($\boxdot$), medium ($\square$), and large ($\blacksquare$); the $CaCO_3$ crystals (x); and the sponge spicules *S. domuncula* ($\blacktriangledown$) and *H. sanguinea* ($\triangledown$). The lines serve only to connect related points and do not necessarily indicate the true shapes of the $E - \gamma$ curves. Error bars indicate one standard error. Specimens were pulled at $\dot{\epsilon} = 0.04$ s^{-1}. The star indicates the mean modulus for unspiculated gelatine. Models containing $\gamma = 0.01$ of *H. sanguinea* spicules were significantly stiffer than gelatine (ANOVA: $F_{[1,13]} = 31.1$, $P < 0.001$), as were models containing $\gamma = 0.01$ of $CaCO_3$ crystals (ANOVA: $F_{[1,13]} = 10.7$, $0.005 < P < 0.01$). The models reinforced with cnidarian spicules of $\gamma = 0.01$ and $\gamma = 0.05$ were not significantly stiffer than gelatine, but did have significantly higher E's than gelatine when $\gamma = 0.15$: *A. digitatum* inner (ANOVA: $F_{[1,14]} = 288.6$, $P < 0.001$), and outer (ANOVA: $F_{[1,13]} = 1076.6$, $P < 0.001$); *S. glaucum* small (ANOVA: $F_{[1,13]} = 413.9$, $P < 0.001$), and large (ANOVA: $F_{[1,13]} = 58.2$, $P < 0.001$); *D. hemprichi* small (ANOVA: $F_{[1,13]} = 4929.6$, $P < 0.001$), medium (ANOVA: $F_{[1,13]} = 83.2$, $P < 0.001$), and large (ANOVA: $F_{[1,15]} = 183.8$, $P < 0.001$).

where r is the fibre radius, σ_F is the fracture strength of the fibre, and τ is the shear stress at the matrix-fibre interface (Wainwright *et al.* 1976). Fibres which are long relative to their transfer length will bear in tension part of the tensile load imposed on the composite. Perhaps the aspect ratio of the sponge spicules is great enough that these spicules act as stiff reinforcing fibres, bearing in tension part of the load on the composite, whereas the other stubbier spicules merely act as filler particles occupying space.

Spicule size and surface area

Small spicules appear to be more stiffening than large ones (Fig. 16). If tissues are reinforced with a given volume fraction of evenly dispersed spicules, smaller expanses of matrix are present between numerous small spicules than between a few large ones. The smaller the spaces between filler particles, the greater will be the local strain amplification within the matrix, the hindrance to rearrangement of matrix molecules, and therefore the stiffness of the composite. Furthermore, small spicules have higher surface-area-to-volume ratios (S/V) than do large spicules; therefore, a given volume fraction of small spicules in a tissue presents more surface area for interaction with
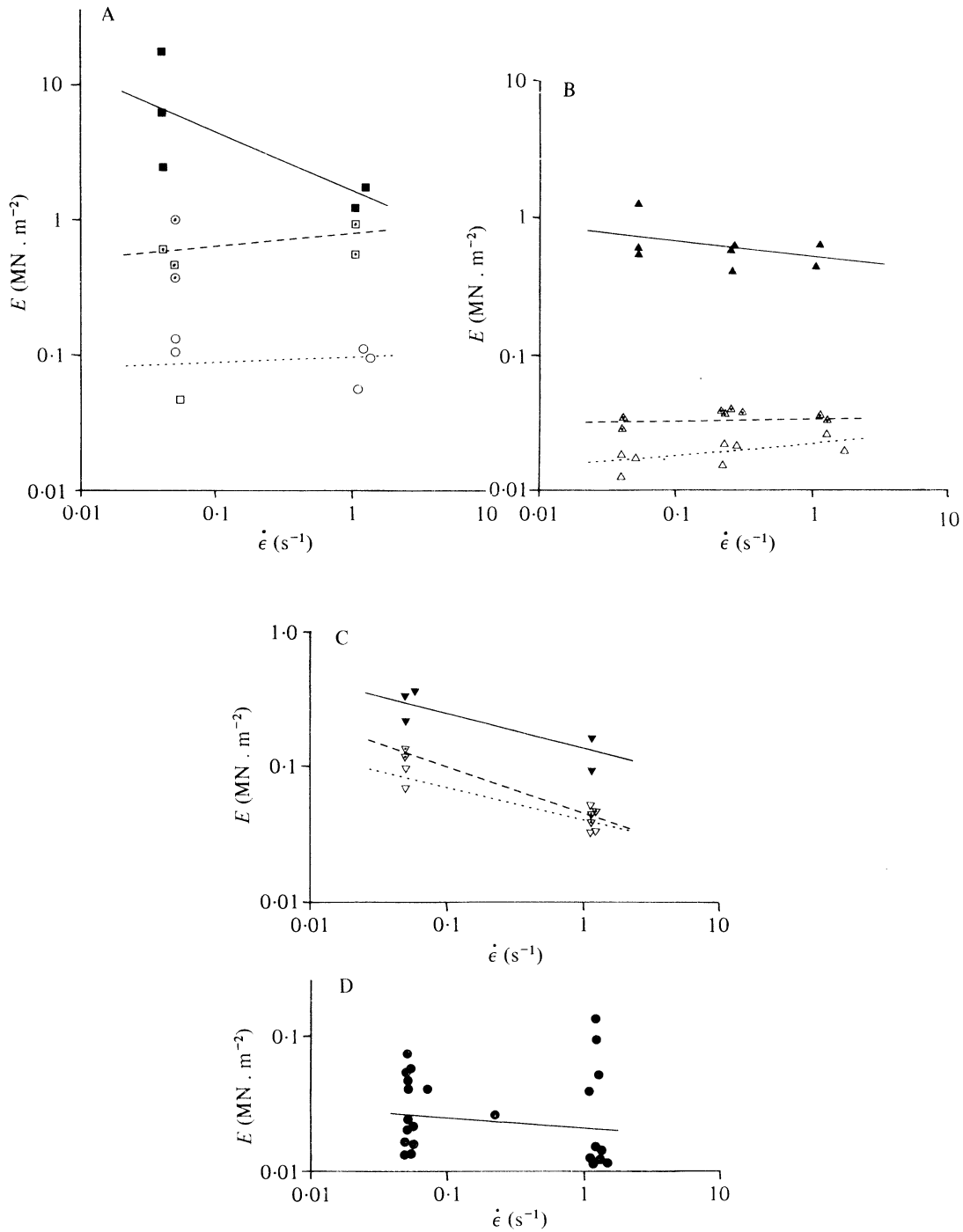
Fig. 14. Graphs of elastic modulus (E) on a logarithmic scale against strain rate ($\dot{\epsilon}$) on a logarithmic scale for model 'tissues' reinforced with (A) sponge spicules: *S. domuncula*, $\gamma = 0.01$ ($\square$), $\gamma = 0.05$ ($\boxdot$), and $\gamma = 0.15$ ($\blacksquare$); *H. sanguinea*, $\gamma = 0.01$ ($\bigcirc$), and $\gamma = 0.05$ ($\odot$); (B) Spicules from *A. digitatum* inner coenenchyme, $\gamma = 0.01$ ($\triangle$), $\gamma = 0.05$ ($\triangle$), and $\gamma = 0.15$ ($\blacktriangle$); (C) CaCO$_3$ crystals, $\gamma = 0.01$ ($\bigtriangledown$), $\gamma = 0.05$ ($\odot$), and $\gamma = 0.15$ ($\bullet$). (D) Graph of E against $\dot{\epsilon}$ for gelatine containing no spicules. Lines represent regressions calculated for models with $\gamma = 0.01$ (dotted lines), $\gamma = 0.05$ (dashed lines), $\gamma = 0.15$ (solid lines in A, B, and C), or $\gamma = 0$ (solid line in D). Although the models reinforced with $\gamma = 0.15$ of spicules appear to be stiffer when pulled slowly than when pulled quickly, the negative correlation between E and $\dot{\epsilon}$ is only significant ($P \leqslant 0.05$) for the three lines in graph C.
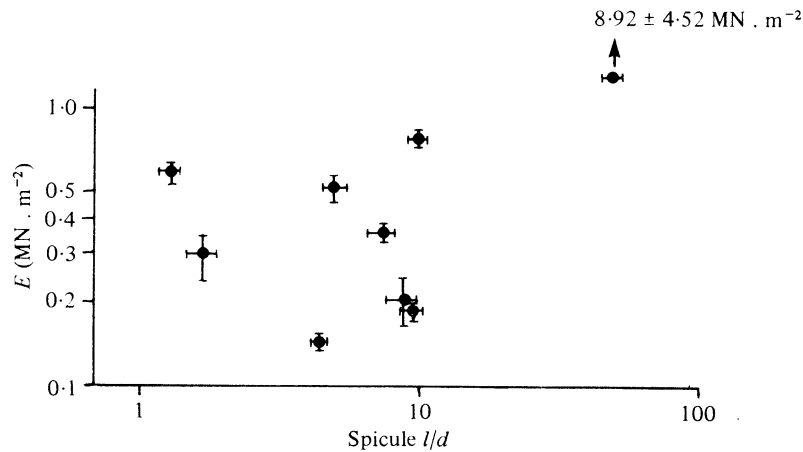
8·92 ± 4·52 MN . m⁻²

Fig. 15. Graph of the mean moduli of elasticity (E) on a logarithmic scale against the mean spicule aspect ratio (l/d) on a logarithmic scale of models reinforced with $\gamma = $ o·15 of various types of spicules. Specimens were pulled at $\dot{e} = $ o·04 s⁻¹. Error bars indicate one standard error. The point at a much higher E and l/d than the others is the mean for models reinforced with spicules from the sponge *S. domuncula*. There is no significant association between spicule l/d and model E, however, for the other models, which contain spicules of low l/d (Kendall Tau: $T = -$o·071, $n = 8$, $P > $ o·8).
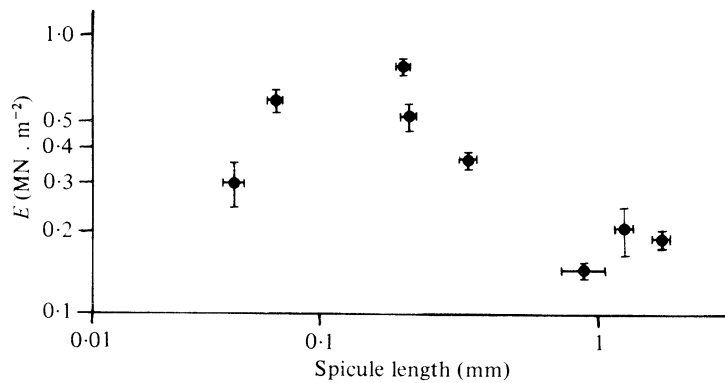

Fig. 16. Graph of the mean elastic moduli (E) on a logarithmic scale against the mean spicule lengths (l) on a logarithmic scale of models reinforced with $\gamma = $ o·15 of various types of spicules. Specimens were pulled at $\dot{e} = $ o·04 s⁻¹. Error bars indicate one standard error. (Specimens reinforced with sponge spicules are not included because sponge spicules appear to act as fibres rather than filler particles.) There is a significant inverse association between l and E (Kendall Tau: $T = -$o·50, $n = 8$, $P = $ o·05).

the matrix than does an equal volume fraction of large spicules. The warts, arms, and spines on spicules increase their S/V, and the E's of model tissues reinforced by a given volume fraction of spicules tend to be greater when the S/V of the spicules is large (Fig. 17). If the stiffening of a tissue depends upon the surface area of spicules available for interacting with the matrix, a particular E can be achieved, for example, by a high volume fraction of large (low (S/V) spicules or by a small volume fraction of small (high S/V) spicules. Indeed, the E of models does increase as the surface area of spicules per volume of tissue (S_{sp}/V_{tis}) increases (Fig. 18).

A greater volume fraction of large (low S/V) spicules is required than of small (high S/V) spicules to achieve a particular surface area of spicules per volume of tissue. Therefore, the spaces between large spicules in a tissue of a given S_{sp}/V_{tis} are
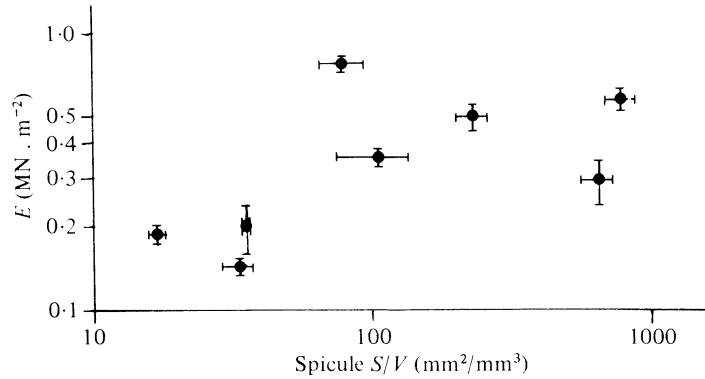
Fig. 17. Graph of the mean elastic moduli (E) on a logarithmic scale against the mean spicule surface-area-to-volume-ratios (S/V) on a logarithmic scale of models reinforced with γ = 0·15 of various types of spicules. Specimens were pulled at $\dot{e}$ = 0·04 s^{-1}. Error bars indicate one standard error. (Specimens reinforced with sponge spicules are not included.) There is a significant direct association between S/V and E (Kendall Tau: T = 0·50, n = 8, P = 0·005).
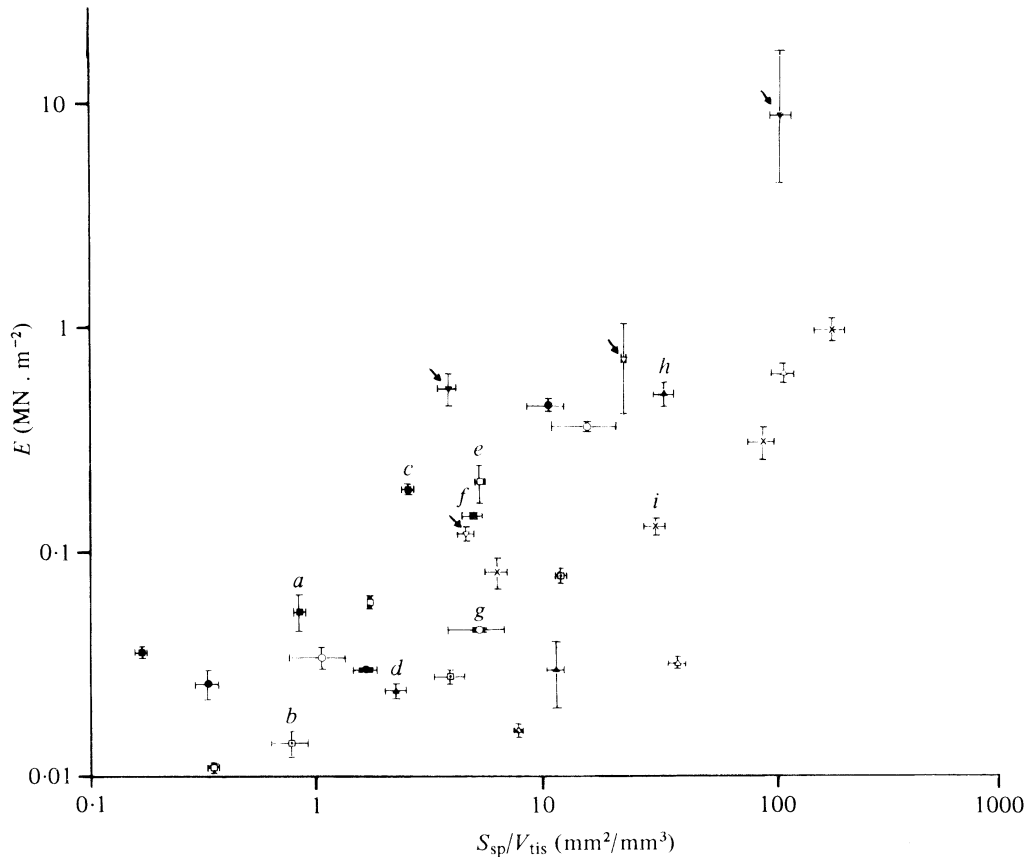

Fig. 18. Graph of the mean elastic moduli (E) on a logarithmic scale against the mean surface area of spicules per volume of tissue (S_{sp}/V_{tis}) on a logarithmic scale of models reinforced with γ = 0·01, 0·05, 0·15, and 0·32 of various types of spicules. Specimens were pulled at $\dot{e}$ = 0·04 s^{-1}. Error bars indicate one standard error. There is a significant direct association between S_{sp}/V_{tis} and E (Kendall Tau: T = 0·53, n = 31, P < 0·005). Symbols are the same as in Fig. 13. Points for specimens containing sponge spicules (indicated by arrows) were not included in the Kendall Tau test. Labelled points are for models reinforced with the following types of spicules: (a) $D.$ $hemprichi$ large, volume fraction (γ) = 0·05, mean length ($\bar{l}$) = 1·72 mm; (b) $D.$ $hemprichi$ small, γ = 0·01, $\bar{l}$ = 0·20 mm; (c) $D.$ $hemprichi$ large, γ = 0·15, $\bar{l}$ = 1·72 mm; (d) $A.$ $digitatum$ inner, γ = 0·01, $\bar{l}$ = 0·21 mm; (e) $D.$ $hemprichi$ medium, γ = 0·15, $\bar{l}$ = 1·23 mm; (f) $S.$ $glaucum$ large, γ = 0·15, $\bar{l}$ = 0·90 mm; (g) $S.$ $glaucum$ small, γ = 0·05, $\bar{l}$ = 0·34 mm; (h) $A.$ $digitatum$ inner, γ = 0·15, $\bar{l}$ = 0·21; (i) CaCO$_3$ crystals, γ = 0·05, $\bar{l}$ = 0·05 mm.

generally smaller than between small spicules in a tissue of the same S_{sp}/V_{tis}. Hence, for a given S_{sp}/V_{tis}, large spicules should be more stiffening than small ones. Comparison of points *a* and *b*, *c* and *d*, *e*, *f*, and *g*, and *h* and *i* in Fig. 18 illustrates that this is so. It appears, therefore, that both the volume spicules occupy in a tissue *and* the surface area of interaction between spicules and matrix are important to the stiffening effect of the spicules.

Stiffness *Biological implications*

Results of this study indicate that spicules stiffen connective tissues in a manner analogous to the stiffening of pliable polymers by filler particles, and that this stiffening effect increases with the volume fraction and surface area of spicules in a tissue. Therefore, I would expect spiculated animals that deform little when subjected to mechanical loads to be reinforced with closely packed spicules and/or with spicules of high S/V. One example consistent with this prediction is that, in a comparative study of two species of *Alcyonium*, Robins (1968) noted that the stiff *A. digitatum* of current-swept habitats were more heavily spiculated than the deformable *A. couchi* of protected habitats. Robins (1968) also noted that the spicules of *A. digitatum* were branched whereas those of *A. couchi* were spindle-shaped.

The distribution of spicules (and therefore of stiffness) within the body of an animal or a colony can affect the way in which the whole structure responds to mechanical loads. For example, the deflexion of a cantilever-like sessile organism or colony, such as a soft coral, when subjected to flowing water (Koehl, 1977*b*) is inversely proportional to the organism's 'flexural stiffness' (the product of E and I, where I is the second moment of area of the cross-section of the cantilever, $I = \int y^2 dA$, where dA is a unit of area at distance y from the axis of bending). Similarly, the twisting of such an organism or colony is inversely proportional to the E and to the polar second moment of area, J, of a cross section ($J = \int y^2 da + \int x^2 dA$, where da and dA are units of area at distances y and x respectively from the axis of torque, and x and y are perpendicular to each other in a plane normal to the axis of torque) (Wainwright *et al.* 1976). Therefore, heavy spiculation (i.e. high E) around the periphery of a fleshy animal or colony is a rigidity-promoting design, whereas heavy spiculation near the centre of such an animal or colony is a flexibility-permitting design. It is not surprising that in *A. digitatum*, which stand upright on exposed rock faces in subtidal areas subjected to rapid currents and/or surge (Robins, 1968; Erwin, 1977), the highest volume fraction of spicules and the spicules with the greatest S/V occur near the outer surface of a colony (Fig. 2B).

The orientation of spicules within an animal or colony also affects the mechanical behaviour of the structure. For example, in hydrostatically-supported cylindrical structures, such as the branches of *D. hemprichi*, the circumferential stresses in the cylinder wall due to the pressure of the contained fluid are twice as big as the longitudinal stresses in the wall (Wainwright *et al.* 1976). If the wall of such a structure is deformable and mechanically isotropic, the cylinder will tend to increase in circumference faster than it lengthens when inflated. The spicules in the walls of *D. hemprichi* tend to be orientated at high angles with respect to the long axis of a branch (Fig. 3D), hence the branch walls are stiffer when pulled circumferentially than when pulled

longitudinally (Fig. 5), and colonies become taller when inflated. Another example of a structure containing anisotropically arranged spicules is the solid stalk of a mushroom-shaped *S. glaucum* colony. Such a stalk, which supports the polyp-bearing capitulum in flowing water, is subjected to bending and/or tensile loads; tensile stresses in the stalk should therefore be greatest in the longitudinal direction, which is the direction in which spicules tend to be orientated (Fig. 3C). It is intriguing to speculate about the possible role of mechanical stresses axes in determining the orientation of spicules in such organisms.

Although big spicules are less stiffening than small ones, many animals contain large spicules. Might there be advantages to being reinforced with big spicules? One might argue that large spicules are more likely than small spicules to irritate the mouths or guts of potential predators. Berquist (1978), however, presents evidence indicating that spicules might not serve as predator-deterrents. The metabolic costs of secreting spicules and connective tissues are not yet known; if it is cheaper to precipitate minerals than to synthesize proteins and mucopolysaccharides, a sessile or sedentary organism (for whom costs of locomotion are unimportant) can perhaps achieve a given stiffness at lower metabolic cost by reinforcing its connective tissue with a high volume fraction of large spicules rather than a low volume fraction of small spicules. Flexibility and extensibility can be features which minimize the breakage of an organism by moving water (Koehl & Wainwright, 1977; Koehl, 1979); for a given volume fraction of spicules, large ones permit more deformation.

Spicule size, shape, and packing can affect the strength and toughness of a tissue as well as its stiffness, as will be discussed elsewhere (Koehl, in preparation). It should also be pointed out that in many animals small spicules are interspersed between large ones; the mechanical consequences of such arrangements have yet to be worked out.

Stress-softening

The spiculated tissues of *A. digitatum* exhibit stress-softening, a behaviour which, has been observed in a few other biological tissues (Chu, 1972, 1973; Vincent, 1975, 1976; Hawkes, 1976). In order to determine whether or not the stress-softening behaviour of a spiculated tissue is important biologically, one must compare the magnitude of the extensions and stresses at which the Mullins effect occurs for a particular tissue with those it experiences *in vivo*.

A. digitatum colonies undergo diurnal (Hickson, 1892; Ceccatty, Buisson & Gargouil, 1963) and seasonal (Hartnoll, 1975) cycles of retraction and expansion; colonies expand as cilia of the siphonoglyphs pump water into the polyps' gastrovascular cavities that extend deep into the coenenchyme. The mean λ_{max} measured for *A. digitatum* inner coenenchyme as the colonies expanded and retracted was 1·29 (S.D. = 0·16, n = 7); Hickson (1895) and Robins (1968) have reported that collected colonies shrink in length by 10–40%, corresponding to λ's between 1·11 and 1·67. Stress-softening can be noted in inner coenenchyme at such λ's (Fig. 6B). The λ's of the outer coenenchyme when colonies undergo such size changes are probably lower than those of the inner coenenchyme because the diameters of the polyps perforating this tissue increases during colony expansion. Vincent (1975, 1976) has suggested that stress-softening materials would be advantageous in biological struc-
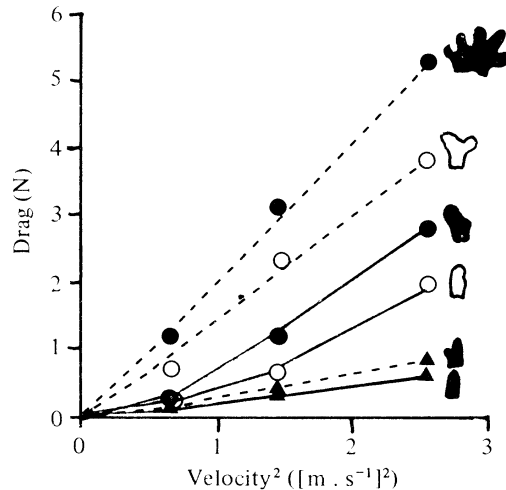
Fig. 19. Graph of drag force (D) against the square of velocity (v^2) for *A. digitatum* colonies towed with their widest axis parallel (solid line) and perpendicular (dashed line) to the direction of water flow. The Reynolds numbers for these colonies at such velocities ranged between 10^4 and 10^5, hence drag force is given by

$$D = (1/2)\rho v^2 A C_D,$$

where ρ is the density of the fluid, A is the projected area of the colony, and C_D is the coefficient of drag. When colony I ($\blacktriangle$) was parallel to the flow, $A = 0.738 \times 10^{-3}\,m^2$ and $C_D = 0.32$ (S.D. $= 0.08$, $n = 3$), and when perpendicular to the flow, $A = 1.160 \times 10^{-3}\,m^2$ and $C_D = 0.44$ (S.D. $= 0.17$, $n = 3$). When colony II ($\bigcirc$) was parallel to the flow, $A = 0.873 \times 10^{-3}\,m^2$ and $C_D = 1.17$ (S.D. $= 0.53$, $n = 3$), and when perpendicular to the flow, $A = 3.049 \times 10^{-3}\,m^2$ and $C_D = 0.184$ (S.D. $= 0.30$, $n = 3$). When colony III ($\bullet$) was parallel to the flow, $A = 1.497 \times 10^{-3}\,m^2$ and $C_D = 0.99$ (S.D. $= 0.54$, $n = 3$), and when perpendicular to the flow, $A = 4.543 \times 10^{-3}\,m^2$ and $C_D = 0.88$ (S.D. $= 0.08$, $n = 3$). The diagram by each line indicates the projected shape of the colony in that orientation.

tures which should maintain their shape, but which should be extendable by small forces. The fleshy colonies of soft corals such as *A. digitatum* appear to be just such structures: they can be inflated by ciliary pumps, but stand up even when cut so that no hydrostatic pressure can be maintained in their gastrovascular cavities.

Stresses in *A. digitatum* coenenchyme *in situ* can be estimated. *A. digitatum* occur on exposed rock faces in subtidal areas subjected to surge and tidal currents; velocities in the vicinity of *A. digitatum* have been measured to be $0.02-0.22\ m.s^{-1}$ (Robins, 1968), and *A. digitatum* are abundant on walls in areas where mainstream velocities can be as high as $3.5\ m.s^{-1}$ (Erwin, 1977). Drag forces on *A. digitatum* colonies of various sizes subjected to a range of flow velocities are plotted in Fig. 19. Small *A. digitatum* colonies are finger-like, whereas larger ones are shaped like planar bloated hands. Although drag forces on and drag-induced stresses in such planar colonies are much lower when colonies are orientated parallel to the flow direction, it is likely that *A. digitatum*, like many other planar organisms (Riedl, 1971), are orientated normal to the predominant current direction; the few colonies I have observed while SCUBA diving were orientated in this way, and the very similar *A. sidereum* have been found to be normal to flow directions (Patterson, 1980). Perhaps this orientation minimizes torsion of the colonies (see Wainwright & Dillon, 1969) and/or enhances the food-capturing ability (see Leversee, 1976) of these planktivorous colonies (Roughshady & Hansen, 1961). Estimates of the maximum tensile stresses in the
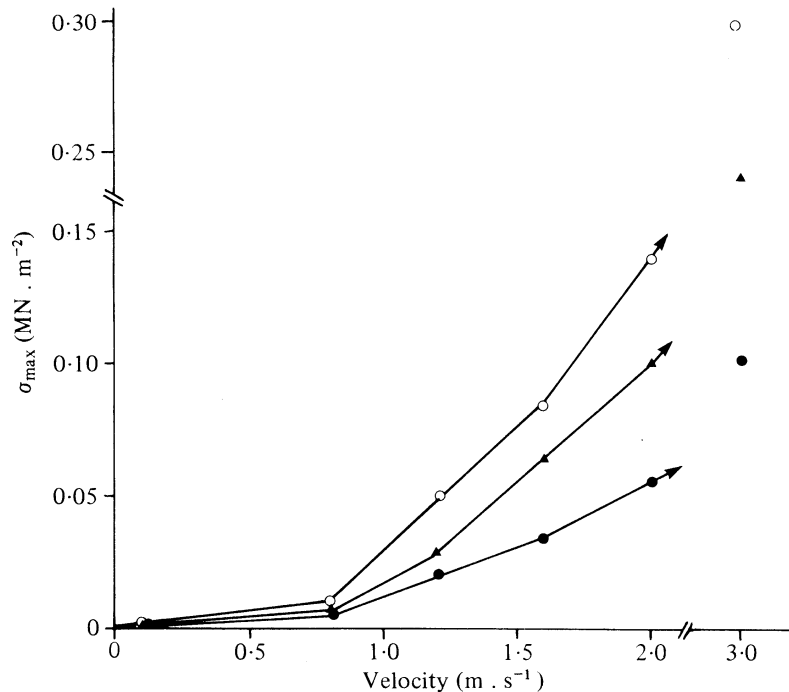
Fig. 20. Graph of calculated estimates of maximum tensile stresses (σ_{max}) in the coenenchyme of the *A. digitatum* colonies plotted in Fig. 19 against the flow velocities which would induce such stresses. Colonies are assumed to be solid beams orientated normal to the direction of water flow. Symbols are the same as those used in Fig. 19. Values for stresses at velocities of 2 m.s^{-1} and 3 m.s^{-1} were calculated using drag forces estimated by extrapolating the drag *vs.* velocity^2 lines in Fig. 19.

coenenchyme of *A. digitatum* colonies when normal to the flow are plotted in Fig. 20.

Even the maximum stresses in colonies exposed to rapid currents are more than an order of magnitude lower that stresses which break coenenchyme (Koehl, in preparation; see Figs. 1, 6, 12). Nonetheless, coenenchyme slowly extends when subjected to low stresses such as these: outer coenenchyme ($n = 7$) subjected to stress of 0·10 MN.m^{-2} (S.D. = 0·04) for 5 h (to simulate the maximum stresses in these tissues in colonies subjected to tidal currents of a few meters per second) extends by $\lambda = 1·34$ (S.D. = 0·15). In contrast, inner coenenchyme, which would *in situ* experience lower stresses than outer coenenchyme, only extends by $\lambda = 1·11$ (S.D. = 0·04, $n = 3$) when subjected to stress of 0·11 MN.m^{-2} (S.D. = 0·07) for 5 h. Such extension test results indicate that the lightly-spiculated inner coenenchyme, which appears to experience less time-dependent Mullins effect than the heavily spiculated outer coenenchyme, may keep the outer coenenchyme from extending as much, when stressed for long times, as it would if it were not continuous with the inner coenenchyme. That co-enenchyme bearing a load extends with time suggests that when *A. digitatum* are subjected to prolonged rapid currents, they may have to maintain their shape by active contraction of muscles and ciliary pumping. The effect of pressure in the polyp gastrovascular cavities in pre-stressing the coenenchyme is not yet known.

The example of *A. digitatum* illustrates the importance of considering the softening as well as the stiffening effects of filler particles when the functional consequences of spiculation are studied.

CONCLUSIONS

The mechanical behaviour of a spicule-reinforced connective tissue depends upon:

(1) The mechanical properties of the pliable connective tissue, which in turn depend upon the amount and orientation of fibres in the tissue, and on the composition and concentration of the amorphous polymer matrix between the fibres (Gosline, 1971; Wainwright *et al.* 1976; Koehl, 1977*a*); (2) the nature of the cross-linking between the spicules, fibres, and amorphous matrix; and (3) the volume fraction, shape, size, and orientation of the spicules. This study, which explored the effects of the latter on the tensile stiffness of spiculated tissues, has revealed several features of such tissues: (1) Spicules increase the stiffness of pliable connective tissues, probably by mechanisms analogous to those by which space-occupying filler particles stiffen deformable polymers – local strain amplification, and interference with molecular rearrangement in response to a load.

(2) The greater the volume fraction of spicules, the stiffer the tissue.

(3) The greater the surface area of spicules per volume of tissue, the stiffer the tissue. Thus, a given volume of spicules of high S/V has a greater stiffening effect than does an equal volume of spicules of low S/V. Furthermore, a high volume fraction of large spicules in a tissue can have the same stiffening effect as a lower volume fraction of smaller spicules.

(4) Spicules that are anisometric in shape have a greater stiffening effect parallel to their long axes.

(5) Spicules with very high aspect ratios appear to act like reinforcing fibres – stress is transferred by shearing from the pliable matrix to the stiff fibres, which thus bear in tension part of the load on the composite.

(6) Spicule-reinforced tissues exhibit stress-softening behaviour, which is more pronounced in heavily-spiculated tissues.

REFERENCES

ALEXANDER, R. McN. (1962). Visco-elastic properties of the body wall of sea anemones. *J. exp. Biol.* **39**, 373–386.

BERQUIST, P. R. (1978). *Sponges.* Berkeley: University of California Press.

BLATZ, P. J. (1969). Application of large deformation theory to the thermomechanical behavior of rubber-like polymers – porous, unfilled, and filled. In *Rheology: Theory and Applications*, vol. 5 (ed. F. R. Eirich), pp. 1–55. New York: Academic Press.

BROWN, C. H. (1975). *Structural Materials in Animals.* New York: Halstead Press.

CECCATTY, M. P., BUISSON, B. & GARGOUIL, Y. M. (1963). Rythmes naturels et reactions motrices chez *Alcyonium digitatum* Linn. et *Veretillum cynomorium* Cuv. *C. r. Séanc. Soc. Biol.* **157**, 616–618.

CHRISTENSEN, R. M. (1979). *Mechanics of Composite Materials.* New York: John Wiley.

CHU, B. M. (1972). Cumulative microdamage model to describe the hysteresis of living tissue. *Ann. biomed. Eng.* **1**, 204–211.

CHU, B. M. (1973). Differences and similarities in the mechanical response of soft living animal tissue and filled polymeric materials. *Biomat., med. dev., art. Org.* **1**, 291–306.

COLLINS, E. A., HOFFMANN, D. J. & SONI, P. L. (1979). Rheology of PVC dispersions. I. Effect of particle size and particle size distribution. *J. Colloid Interface Sci.* **71**, 21–29.

CURREY, J. D. (1970). *Animal Skeletons.* New York: St Martin's Press.

DICKIE, R. A. (1977). The viscoelastic properties of particulate polymeric composites. In *Polymer Engineering Composites* (ed. M. O. W. Richardson), pp. 155–195. London: Applied Science Publishers.

DINGERKUS, G. & UHLER, L. D. (1977). Enzyme clearing of alcian blue stained whole small vertebrates for demonstration of cartilage. *Stain Technol.* **52**, 229–232.

ERWIN, D. G. (1977). A diving survey of Strangford Lough: The benthic communities and their relation to substrate – a preliminary account. In *Biology of Benthic Organisms* (ed. B. F. Keegan, P. O. Ceidigh and P. J. S. Boaden), pp. 215–223. Oxford: Pergamon Press.

EYLERS, J. P. (1976). Aspects of skeletal mechanics of the starfish *Asterias forbesii. J. Morph.* **149**, 353–367.

FARRIS, R. J. (1972). The stress–strain behavior of mechanically degradable polymers. In *Polymer Networks* (ed. A. J. Chompff and S. Newman), pp. 341–394. New York: Plenum Press.

FEDORS, R. F. & LANDEL, R. F. (1975). Mechanical behavior of SBR-glass bead composites. *J. Polymer Sci.* **13**, 579–597.

FERRY, J. D. (1970). *Viscoelastic Properties of Polymers,* 2nd ed. New York: John Wiley.

GARRONE, R., HUC, A. & JUNQUA, S. (1975). Fine structure and physiochemical studies on the collagen of the marine sponge *Chondrosia reinformis* Nardo. *J. Ultratrurct. Res.* **52**, 261–275.

GIBBONS, J. D. (1976). *Nonparametric Methods for Quantitative Analysis.* New York: Holt, Rinehart and Winston.

GOSLINE, J. M. (1971). Connective tissue mechanics of *Metridium senile.* II. Visco-elastic properties and macromolecular model. *J. exp. Biol.* **55**, 775–795.

HARTNOLL, R. G. (1975). The annual cycle of *Alyconium digitatum.* Estuarine *Coastal mar. Sci.* **3**, 71–78.

HAWKES, R. (1976). *Carchesium* stalk fibrillar matrix as a highly filled polymer network. *J. cell Physiol.* **90**, 31–40.

HICKSON, S. J. (1892). Some preliminary notes on the anatomy and habits of *Alcyonium digitatum. Proc. Camb. phil. Soc.* **7**, 305–308.

HICKSON, S. J. (1895). The anatomy of *Alcyonium digitatum. Q. Jl microsc. Sci.* **37**, 343–388.

HICKSON, S. J. (1901). *Alcyonium. L.M.B.C. Mem. typ. Br. mar. Pl. Anim.* **5**, 1–22.

JACKSON, J. B. C. (1977). Competition on marine hard substrata: The adaptive significance of solitary and colonial strategies. *Am. Nat.* **111**, 743–767.

JONES, W. C. (1970). The composition, development, form and orientation of calcareous sponge spicules. *Symp. zool. Soc. Lond.* **25**, 91–123.

JUNQUA, S., FAYOLLE, J. & ROBERT, L. (1975). Structural glycoproteins from sponge intercellular matrix. *Comp. Biochem. Physiol.* **50** B, 305–309.

KOEHL, M. A. R. (1977a). Mechanical diversity of the connective tissue of the body wall of sea anemones. *J. exp. Biol.* **69**, 107–125.

KOEHL, M. A. R. (1977b). Mechanical organization of cantilever-like sessile orangisms: Sea anemones. *J. exp. Biol.* **69**, 127–142.

KOEHL, M. A. R. (1977c). Water flow and the morphology of zooanthid colonies. *Proc. 3rd Int. Coral Reef Symp.,* vol. 1: *Biol.,* pp. 437–444.

KOEHL, M. A. R. (1979). Stiffness or extensibility of intertidal algae: A comparative study of modes of withstanding wave action. *J. Biomech.* **12**, 634.

KOEHL, M. A. R. & WAINWRIGHT, S. A. (1977). Mechanical adaptations of a giant kelp. *Limnol. Oceanogr.* **22**, 1067–1071.

KOTANI, T. & STERNSTEIN, S. S. (1972). Birefringence analysis of inhomogeneous swelling in filled elastomers. In *Polymer Networks* (ed. A. J. Chompff and S. Newman), pp. 273–291. New York: Plenum.

KRAUS, G. (ed.) (1965). *Reinforcement of Elastomers.* New York: Interscience.

LEPIE, A. & ADICOFF, A. (1972). Dynamic mechanical behavior of highly filled polymers. Dewetting effects. *J. appl. Polym. Sci.* **16**, 1155–1166.

LEVERSEE, G. J. (1976). Flow and feeding in fan-shaped colonies of the gorgonian coral, *Leptogorgia. Biol. Bull. mar. biol. Lab., Woods Hole* **151**, 344–356.

MARISCAL, R. N. (1974). Scanning electron microscopy of the sensory surface of the tentacles of sea anemones and corals. *Z. Zellforsch. mikrosk. Anat.* **14**, 149–156.

MARK, H. F. (1970). New composites – Morphology and properties. *Appl. Polym. Symp.* **15**, 3–8.

MASCIA, L. (1974). *The Role of Additives in Plastics.* London: Edward Arnold.

MULLINS, L. (1963). Effects of fillers in rubbers. In *The Chemistry and Physics of Rubber-like Substances* (ed. L. Bateman), pp. 301–328. London: Maclaren.

MULLINS, L. (1980). Theories of rubber-like elasticity and the behaviour of filled rubber. *Soc. exp. Biol. Symp.* **34**, 273–287.

MUZIK, K. & WAINWRIGHT, S. A. (1977). Morphology and habitat of five Fijian sea fans. *Bull. mar. Sci.* **27**, 308–337.

NICODEMO, L. & NICOLAIS, L. (1974a). Filler effect on the relaxation time of fibre suspensions in polymeric solutions. *Polymer* **15**, 589–592.

NICODEMO, L. & NICOLAIS, L. (1974b). Viscosity of bead suspensions in polymeric solutions. *J. appl. Polym. Sci.* **18**, 2809–2818.

NICODEMO, L., NICOLAS, L. & LANDEL, R. F. (1974). Shear rate dependent viscosity of suspensions in Newtonian and non-Newtonian liquids. *Chem. Engng. Sci.* **29**, 729–735.

PAINE, R. T. (1971). Measurement and application of the calorie to ecological problems. *A. Rev. Ecol. Syst.* **2**, 145–164.

PANTIN, C. F. A. (1964). *Notes on Microscopical Technique for Zoologists.* Cambridge: Cambridge University Press.

PATTERSON, M. R. (1980). Hydromechanical adaptations in *Alcyonium sidereum.* In *Biofluid Mechanics,* vol. 2 (ed. D. Schneck), pp. 183–201. New York: Plenum Press.

REIF, W.-E. & ROBINSON, J. A. (1976). On functional morphology of the skeleton in lychnisc sponges (Porifera, Hexactinellida). *Paläont. Z.* **50**, 57–69.

RIEDL, R. J. (1971). Water movement. In *Marine Ecology,* vol. 1, Pt. 2 (ed. O. Kinne), pp. 1085–1088, 1124–1156. London: Wiley-Interscience.

ROBINS, M. W. (1968). The ecology of *Alcyonium* species in the Scilly Isles. *Underwater Assoc. Report,* 67–71.

ROUSHADY, H. M. & HANSEN, V. K. (1961). Filtration of phytoplankton by the Octocoral *Alcyonium digitatum* L. *Nature, Lond.* **190**, 649–650.

SNEDECOR, G. W. (1956). *Statistical Methods,* 5th ed. Ames. Iowa: Iowa State College Press.

SOKAL, R. R. & RHOLF, F. J. (1969). *Biometry.* San Francisco: W. H. Freeman.

TITOW, W. V. & LANHAM, B. J. (1975). *Reinforced Thermoplastics.* London: Applied Science Publishers.

VINCENT, J. F. V. (1975). Locust oviposition: Stress softening of the extensible intersegmental membranes. *Proc. R. Soc. Lond.* A **188**, 189–201.

VINCENT, J. F. V. (1976). Design for living – the elastic-sided locust. In *The Insect Integument* (ed. H. R. Hepburn), pp. 401–419. Elsevier.

VIIDIK, A. (1972). Functional properties of collagenous tissues. *Int. Rev. connective Tissue Res.* **6**, 127–215.

WAINWRIGHT, S. A., BIGGS, W. D., CURREY, J. D. & GOSLINE, J. M. (1976). *Mechanical Design in Organisms.* London: Edward Arnold.

WAINWRIGHT, S. A. & DILLON, J. R. (1969). On the orientation of sea fans (genus *Gorgonia*). *Biol. Bull. mar. biol. Lab., Woods Hole* **136**, 130–139.

WAKE, W. C. (ed.) (1971). *Fillers for Plastics.* London: Iliffe Books.

WASSERSUG, R. J. (1976). A procedure for differential staining of cartilage and bone in whole formalin-fixed vertebrates. *Stain Technol.* **51**, 131–134.

WEAST, R. C. & ASTLE, M. J. (eds.) (1978). *CRC Handbook of Chemistry and Physics,* 59th Edition. West Palm Beach, Fla.: CRC Press.